

# All Things Retarded: Radiation-Reaction in Worldline Quantum Field Theory

GUSTAV UHRE JAKOBSEN,<sup>1,2,3</sup> GUSTAV MOGULL,<sup>1,2,3</sup>  
JAN PLEFKA<sup>1,3</sup> AND BENJAMIN SAUER<sup>1</sup>

<sup>1</sup>*Institut für Physik und IRIS Adlershof, Humboldt-Universität zu Berlin,  
Zum Großen Windkanal 2, D-12489 Berlin, Germany*

<sup>2</sup>*Max-Planck-Institut für Gravitationsphysik (Albert-Einstein-Institut)  
Am Mühlenberg 1, D-14476 Potsdam, Germany*

<sup>3</sup>*Kavli Institute for Theoretical Physics, University of California,  
Santa Barbara, CA 93106, USA*

{gustav.uhre.jakobsen@physik.hu-berlin.de, gustav.mogull@aei.mpg.de,  
jan.plefka@hu-berlin.de, benjamin.sauer@hu-berlin.de}

## Abstract

We exhibit an initial-value formulation of the worldline quantum field theory (WQFT) approach to the classical two-body problem in general relativity. We show that the Schwinger-Keldysh (in-in) formalism leads to purely retarded propagators in the evaluation of observables in the WQFT. Integration technology for retarded master integrals is introduced at third post-Minkowskian (3PM) order. As an application we compute the complete radiation-reacted impulse and radiated four momentum for the scattering of two non-spinning neutron stars including tidal effects at 3PM order, as well as the leading (2PM) far-field gravitational waveform.

# Contents

<b>1</b>	<b>Introduction</b>	<b>1</b>
<b>2</b>	<b>In-in formalism for WQFT</b>	<b>4</b>
2.1	One-point functions in the in-out formalism	5
2.2	One-point functions in the in-in formalism	6
2.3	In-in one-point functions in background field theory	8
2.4	In-in formalism for WQFT: observables	11
2.5	In-in formalism for WQFT: free energy	12
<b>3</b>	<b>Retarded integrals</b>	<b>13</b>
3.1	Linear identities	15
3.2	Canonical bases	16
3.3	Method of regions	18
3.4	Mushroom integrals	20
3.5	Integral expressions	22
<b>4</b>	<b>Radiation-reacted tidal effects</b>	<b>23</b>
4.1	Impulse	24
4.2	Scattering angle	27
4.3	Radiated momentum	28
4.4	Waveform	29
<b>5</b>	<b>Conclusions</b>	<b>32</b>
<b>A</b>	<b>In-in propagator matrix</b>	<b>34</b>

## 1 Introduction

The gravitational two-body problem lies at the origin of physics as a scientific discipline [1]. The Newtonian case is well known to be integrable and supports bound or unbound orbits depending on the conserved energy of the system. In general relativity (GR) the same is true in principle, yet the problem is more complicated due to the loss of energy and (angular) momentum through gravitational radiation. In bound systems the continuous emission of gravitational radiation leads to an ever-shrinking inspiral followed by a merger of the two massive objects — black holes, neutron stars or stars. With the gravitational waves emitted by such violent encounters now routinely being detected by the LIGO-Virgo-KAGRA observatories [2], a new era of gravitational wave (GW) astronomy has begun. This calls for high precision predictions of the emitted waveforms in binary encounters depending on the source’s parameters.

Due to the non-linearity of Einstein’s equations and radiative effects exact results are out of reach, and one is forced to use approximate perturbative or numerical approaches. In bound systems the inspiral phase typically runs over many cycles, and so perturbative methods are preferable: one often uses a *post-Newtonian* (PN) expansion in Newton’s constant  $G$  and relative velocity  $v$  (with  $\frac{Gm}{r} \sim v^2 \ll 1$ ), which works well for near-circular orbits [3–8] [9–17]. On the other hand, for unbound systems — i.e. gravitational scattering events, in which the two massive bodies fly past each other — the *post-Minkowskian* (PM) weak-field expansion in powers of Newton’s constant  $G$  is more natural. While the non-periodic gravitational Bremsstrahlung produced by such scattering events appears to be out of reach of current-generation GW detectors, it may be detectable in the third generation of GW detectors [18–22]. The close relationship between bound and unbound two-body systems also allows one to recycle scattering observables into useful input for the bound problem [23–25]. This is especially useful for highly elliptic bound orbits where the relative velocity  $v$  is large at the point of closest approach [22].

In an effective field theory (EFT) setting, well-separated black holes (BHs) or neutron stars (NSs) can be idealized as two massive point particles moving on trajectories  $x_i^\mu(\tau)$  coupled to gravity. Finite-size and tidal effects are included by coupling an infinite series of higher-dimensional operators to the particle’s worldline theory with free Wilson coefficients (Love numbers)  $c_{E^2/B^2}^{(i)}$ . Using the Polyakov formulation with einbein  $e$  the one-dimensional worldline theory reads

$$S_{\text{pm}}^{(i)} = -m_i \int d\tau_i \left[ \frac{1}{2e} g_{\mu\nu}(x_i) \dot{x}_i^\mu(\tau_i) \dot{x}_i^\nu(\tau_i) + \frac{e}{2} + \frac{c_{E^2}^{(i)}}{e^3} E_{\mu\nu}^{(i)} E^{(i)\mu\nu} + \frac{c_{B^2}^{(i)}}{e^3} B_{\mu\nu}^{(i)} B^{(i)\mu\nu} + \dots \right],$$

where we have included the first layer of tidal effects which are quadratic in the Riemann tensor and quartic in  $\dot{x}_i^\mu$  — see eq. (4.1) for a definition. The complete gravitational field theory consists of these two point-mass worldline actions  $S_{\text{pm}}^{(i)}$  ( $i = 1, 2$ ) coupled to the four-dimensional bulk Einstein-Hilbert action  $S_{\text{EH}}$ .

Expanding the metric around a flat Minkowski vacuum,  $g_{\mu\nu}(x) = \eta_{\mu\nu} + \kappa h_{\mu\nu}(x)$  with  $\kappa = \sqrt{32\pi G}$ , one solves the resulting equations of motion for the trajectories  $x_i^\mu(\tau_i)$  and the graviton waveform  $h_{\mu\nu}(x)$  perturbatively in  $G$ . In a scattering scenario the initial boundary conditions are straight-line trajectories of the two bodies,  $x_i^\mu = b_i^\mu + v_i^\mu \tau_i$ , with no incoming radiation  $h_{\mu\nu} = 0$ . Provided the impact parameter is large compared with the intrinsic size of the massive bodies, i.e.  $|\mathbf{b}| = |\mathbf{b}_1 - \mathbf{b}_2| \gg Gm_i$ , the weak-field expansion and point-particle approximations are valid. Key observables in the gravitational scattering problem are: (i) the waveform  $h_{\mu\nu} = \frac{f(t, \vec{x})}{r} + \dots$  in the far zone  $r \gg |\mathbf{b}|$ , (ii) the impulse or momentum deflection  $\Delta p_i^\mu := m_i [\dot{x}_i^\mu(\tau = +\infty) - \dot{x}_i^\mu(\tau = -\infty)]$  of the  $i$ ’th body (which also contains the scattering angle  $\theta$ ), and for spinning bodies (iii) the “spin kick”  $\Delta a_i^\mu$ , i.e. the change of the  $i$ ’th body’s spin vector. These quantities also encode the total energy, momentum and angular momentum dissipated via gravitational radiation (Bremsstrahlung). A special feature of gravity

is that the field  $h_{\mu\nu}$  does not relax to zero after the scattering event; instead, it takes on a new finite value — the memory effect. This traditional GR approach of solving the equations of motion perturbatively has been used to establish the leading-order (LO) gravitational waveform [26–29], the deflection angle up to 2PM [7, 8, 30] and the explicit trajectory up to 2PM order [31] — see also recent work on the electromagnetic analogue at 3PM order [32].

Quantum field theory (QFT) techniques employing a classical limit of the perturbatively evaluated path integral have also proven themselves highly effective. Initially introduced for the computation of an effective worldline action in the PN expansion [9–17] — see [33, 34] for reviews — these have now been successfully extended to the scattering problem in a PM expansion [35]. Conservative observables including spin effects have been computed at 2PM order [36], at 3PM order including tidal effects [37, 38] and at 4PM order [39, 40]. In this worldline EFT approach graviton fluctuations  $h_{\mu\nu}$  are integrated out of the path integral of the above action,  $S_{\text{EH}} + \sum_{i=1}^2 S_{\text{pm}}^{(i)}$ , yielding an effective action  $\Gamma[x_i]$  describing only the massive bodies’ positions. The equations of motion for  $\Gamma[x_i]$  are then perturbatively solved in  $G$ , yielding the desired deflection observables. Radiative observables at 3PM order have also been derived from the LO waveform [41–44]. However, a systematic inclusion of radiation-reaction effects at higher PM orders requires the introduction of a Schwinger-Keldysh “in-in” path-integral formalism [45, 46], as the classical problem to be solved is an initial-value problem.

In a series of papers involving three of the present authors we have developed an efficient extension to the worldline EFT approach known as *worldline quantum field theory* (WQFT) [47–51]. WQFT implements the philosophy of the modern scattering amplitudes program [52–56] by directly computing *on-shell observables*: translating this to the worldline EFT calls for integrating out fluctuations of the worldline fields  $x_i^\mu$ . All classical observables, including the impulse, spin kick and waveform are derived from *tree-level one-point functions* in WQFT. Indeed, the one-point functions directly yield the desired solutions of the classical equations of motion of the system once the correct boundary conditions are implemented. In essence, the WQFT formalism provides an efficient diagrammatic framework for solving the classical equations of motion of the spinning gravitational two-body system perturbatively. Moreover, in WQFT the spin degrees of freedom are captured by introducing anti-commuting worldline fields that display an extended supersymmetry [50]. Using this state-of-the-art results for the waveform with [49] and without spin [48] as well as the 3PM impulse and spin kick up to quadratic order in spin [51] have been established. Further works have addressed light bending [57], the double copy [58] and applications to the eikonal phase [59].

In this paper we describe how the WQFT systematically incorporates radiation-reaction effects by implementing the Schwinger-Keldysh “in-in” path-integral formalism. The outcome is to be expected, and was already implied in our previous

works: when computing tree-level one-point functions using the WQFT in-in formalism one uses exactly the same Feynman rules as the WQFT in-out formalism, but with *retarded* propagators pointing towards the outgoing line. This follows from a simple diagrammatic argument explained in section 2. We therefore extend modern Feynman loop integration technology to handle retarded propagators, initiating this program in section 3 for the specific case of a 3PM integral family. In section 4 we also apply the complete WQFT formalism to compute non-spinning radiative observables (impulse, scattering angle, waveform) at 3PM *including tidal effects*. By contrast, in the traditional worldline EFT approach one goes through the intermediate stage of an effective action and a laborious separation into advanced and retarded propagators in a doubled field approach is required.

A complementary and rapidly developing alternative approach to the classical gravitational scattering problem is based on scattering amplitudes [60–68]. Here, massive scalar fields are the avatars of spinless BHs or NSs, and one obtains scattering data from  $2 \rightarrow 2$  amplitudes taken in the classical  $\hbar \rightarrow 0$  limit. The innovations of the scattering amplitude program for constructing tree- and loop-level amplitudes in perturbatively quantized GR have recently enabled quick progress to higher PM orders. The conservative effective potential has been established at 3PM [64–66] and recently at 4PM order [69, 70] in the non-spinning case. The scattering of higher-spin fields may also be used to emulate the compact objects’ spin [71–77]. However, here the inclusion of radiation-reaction effects here poses a challenge [67, 78–81], and so far the complete impulse  $\Delta p_i^\mu$  has only been produced in the non-spinning case. Radiative corrections to the 3PM scattering angle  $\theta$  have, nevertheless, been produced to arbitrary orders in spin [82]. The KMOC formalism addresses this problem by introducing an in-in style formalism in this context [83–86], but matching to the worldline EFT Wilson coefficients remains subtle. Recently, amplitude techniques were also successfully applied to the radiation-reaction problem (tail effect) in the PN approach [87].

Another recently developed approach uses heavy-particle effective theories (HEFTs) to describe the massive bodies [88, 89]. State-of-the-art results here include the spinless 3PM scattering angle [89], spinning results with tidal effects [90] and at 2PM with arbitrary spin orders of one particle [91].

*Note added:* While finalizing this paper we became aware of the work [92] which overlaps with some of our results.

## 2 In-in formalism for WQFT

It is a textbook QFT result that the effective action  $\Gamma[\phi]$  — computable through a Legendre transform of the generating functional  $W[J]$ , or by the background field method — is identical to the classical action at tree level. Moreover, the one-point

function  $\langle \hat{\phi}(x) \rangle$  solves the equations of motion  $\frac{\delta \Gamma[\phi]}{\delta \phi} \Big|_{\phi=\langle \hat{\phi}(x) \rangle} = 0$  in the absence of sources  $J$ . This relation is the basis for our use of QFT to efficiently solve classical physics problems. However, the one-point function  $\langle \hat{\phi}(x) \rangle$  in the standard “in-out” path integral formalism is the solution to a boundary value problem; not the initial-value problem that is required in a classical setting. This is because the in-out one-point function  $\langle \hat{\phi}(x) \rangle$  — as opposed to its notation — is not a true expectation value of the field operator  $\hat{\phi}(x)$ . Rather, it is the matrix element of  $\hat{\phi}(x)$  between the in-vacuum and the out-vacuum state to which the in-vacuum has evolved, and these two states need not be identical. Realization of the true expectation value of the field operator in the in-vacuum state as a one-point function is achieved using the Schwinger-Keldysh “in-in” path integral formalism [45, 46], which we shall now review — following closely the pedagogical expositions found in refs. [13, 93].

## 2.1 One-point functions in the in-out formalism

Let us first review a few important details regarding the in-out formalism. To simplify the discussion we consider a free massless scalar field theory coupled to an external physical source  $Q(x)$

$$S[\phi] = \frac{1}{2} \int d^4x \partial_\mu \phi \partial^\mu \phi + S_{\text{int}}[\phi; Q]. \quad (2.1)$$

The WQFT analogues of  $\phi$  are the fluctuating “quantum” fields on the worldlines  $z_i^\mu(\tau)$  and the graviton  $h_{\mu\nu}(x)$  in the bulk, while the source  $Q$  emerges from the background configurations  $b_i^\mu + v_i^\mu \tau$  on the worldlines that couple non-linearly to  $z_i^\mu$  and  $h_{\mu\nu}$ . However, let us for now consider an arbitrary interaction term  $S_{\text{int}}[Q, \phi]$  that depends on an external source  $Q(x)$  in an unspecified manner.

In the interaction picture the state of the system is time dependent. Let  $|\Psi\rangle$  be the state of the system in the infinite past ( $T = -\infty$ ), when the interaction and Heisenberg picture are taken to coincide. The time evolution of the state vector in the interaction picture is governed by the interaction Hamiltonian  $\hat{H}_{\text{int}}$ ,  $|\Psi(t)\rangle = \hat{U}(t, -\infty)|\Psi\rangle$ , with the time-evolution operator

$$\hat{U}(T', T) = \mathcal{T} \exp \left[ \frac{i}{\hbar} \int_T^{T'} dt \int d^3x \hat{H}_{\text{int}}[Q(t, \mathbf{x}), \hat{\phi}_I(t, \mathbf{x})] \right]. \quad (2.2)$$

$\mathcal{T}$  denotes time ordering and  $\hat{\phi}_I(t, \mathbf{x})$  is the field operator in the interaction picture (see e.g. ref. [94] chapter 7). It is related to the field in the Heisenberg picture  $\hat{\phi}_H(t, \mathbf{x})$  via

$$\hat{\phi}_I(t, \mathbf{x}) = \hat{U}(t, -\infty) \hat{\phi}_H(t, \mathbf{x}) \hat{U}(-\infty, t). \quad (2.3)$$

We now add an auxiliary external linear source  $J(x)$  to the system

$$\hat{U}_J(T', T) = \mathcal{T} \exp \left[ \frac{i}{\hbar} \int_T^{T'} dt \int d^3x \left( \hat{H}_{\text{int}}[Q, \hat{\phi}_I] + J(x) \hat{\phi}_I(x) \right) \right]. \quad (2.4)$$

The vacuum transition amplitude in the presence of sources has the in-out path-integral representation

$$\langle 0|\hat{U}_J(\infty, -\infty)|0\rangle = \int D\phi \exp\left\{\frac{i}{\hbar}\left(S[\phi] + \int d^4x J(x)\phi(x)\right)\right\} =: e^{\frac{i}{\hbar}W[J]}, \quad (2.5)$$

Here,  $|0\rangle$  represents the vacuum state in the infinite past when the interactions are assumed to turn off. The in-out one-point function of the Heisenberg field is

$$\begin{aligned} \langle \hat{\phi}_H(t, \mathbf{x}) \rangle_{\text{in-out}} &:= \left. \frac{\delta W}{\delta J(t, \mathbf{x})} \right|_{J=0} = \langle 0|\hat{U}(\infty, t)\hat{\phi}_I(t, \mathbf{x})\hat{U}(t, -\infty)|0\rangle \\ &= \langle 0|\hat{U}(\infty, -\infty)\hat{\phi}_H(t, \mathbf{x})|0\rangle. \end{aligned} \quad (2.6)$$

This simple example illustrates that we have *not* evaluated the vacuum expectation value of the Heisenberg field operator, but rather the matrix element between the in-vacuum  $|0\rangle$  and the state  $\hat{U}(-\infty, \infty)|0\rangle$ , i.e. the out-vacuum. Hence, the tree-level one-point function  $\langle \hat{\phi}_H(t, \mathbf{x}) \rangle_{\text{in-out}}$  cannot be identified with the classical field configuration  $\phi_{\text{class}}(x)$ , which should be given by a vacuum expectation value of the field operator in the Heisenberg picture,  $\langle 0|\hat{\phi}_H(t, \mathbf{x})|0\rangle$ .

This is easily verified by specializing the interacting piece of the action (2.1) to a linear term  $S_{\text{int}}[Q, \phi] = \int d^4x Q(x)\phi(x)$ . Then the path integral of eq. (2.6) may be performed exactly, yielding

$$\langle \hat{\phi}_H(x) \rangle_{\text{in-out}} = \int d^4y D_F(x-y) Q(y) \quad (2.7)$$

with the Feynman propagator (or Green's function)  $D_F(x)$ . While this solves the classical equations of motion  $\partial^2\phi(x) = Q(x)$  emerging from (2.1) (as it should), it is not the causal solution one usually seeks for in classical physics: for this, we instead need a *retarded* propagator  $D_{\text{ret}}(x-y)$ .

## 2.2 One-point functions in the in-in formalism

The Schwinger-Keldysh in-in formalism is designed to yield a one-point function that *is* a true expectation value of the field in the Heisenberg picture, i.e. we demand that

$$\langle \hat{\phi}_H(t, \mathbf{x}) \rangle_{\text{in-in}} := \langle 0|\hat{\phi}_H(t, \mathbf{x})|0\rangle = \langle 0|\hat{U}(-\infty, t)\hat{\phi}_I(t, \mathbf{x})\hat{U}(t, -\infty)|0\rangle. \quad (2.8)$$

To achieve this, we introduce a generating functional  $W[J_1, J_2]$  depending on two auxiliary external linear sources that generalizes eq. (2.5):

$$e^{\frac{i}{\hbar}W[J_1, J_2]} = \langle 0|\hat{U}_{J_2}(-\infty, \infty)\hat{U}_{J_1}(\infty, -\infty)|0\rangle. \quad (2.9)$$

Note that we maintain only one external source field  $Q$ . The in-vacuum is evolved to the infinite future in the presence of sources  $J_1$ , and  $Q$  is then evolved backwards

in time to the infinite past in the presence of  $J_2$  and  $Q$ . One may then express the expectation value eq. (2.8) in two equivalent ways:

$$\begin{aligned} \frac{\delta W[J_1, J_2]}{\delta J_1(t, \mathbf{x})} \Big|_{J_i=0} &= \langle 0 | \hat{U}(-\infty, \infty) \hat{U}(\infty, t) \hat{\phi}_I(t, \mathbf{x}) \hat{U}(t, -\infty) | 0 \rangle \\ &= \frac{\delta W[J_1, J_2]}{\delta J_2(t, \mathbf{x})} \Big|_{J_i=0} = \langle 0 | \hat{U}(-\infty, t) \hat{\phi}_I(t, \mathbf{x}) \hat{U}(t, \infty) \hat{U}(\infty, -\infty) | 0 \rangle \\ &= \langle 0 | \hat{U}(-\infty, t) \hat{\phi}_I(t, \mathbf{x}) \hat{U}(t, -\infty) | 0 \rangle = \langle \hat{\phi}_H(t, \mathbf{x}) \rangle_{\text{in-in}}. \end{aligned} \quad (2.10)$$

The generating functional  $W[J_1, J_2]$  has a path integral representation upon doubling the fields. It is established by inserting the unit operator  $\mathbf{1} = \sum_{|\psi\rangle} |\psi\rangle \langle\psi|$  into eq. (2.9) using eq. (2.5):

$$\begin{aligned} e^{\frac{i}{\hbar} W[J_1, J_2]} &= \sum_{|\psi\rangle} \langle 0 | \hat{U}_{J_2}(-\infty, \infty) |\psi\rangle \langle\psi| \hat{U}_{J_1}(\infty, -\infty) | 0 \rangle \\ &= \int \mathcal{D}[\phi_1, \phi_2] \exp \left\{ \frac{i}{\hbar} \left[ S[\phi_1] - S[\phi_2] + \int d^4x \left( J_1(x) \phi_1(x) - J_2(x) \phi_2(x) \right) \right] \right\}. \end{aligned} \quad (2.11)$$

The  $\phi_1$  field propagates forward in time, the  $\phi_2$  field backwards. Importantly, in the path integral above the two fields are linked via the boundary condition at future infinity  $\phi_1(t = +\infty, \mathbf{x}) = \phi_2(t = +\infty, \mathbf{x})$ , while at past infinity both fields vanish  $\phi_1(t = -\infty, \mathbf{x}) = \phi_2(t = -\infty, \mathbf{x}) = 0$ . This is a consequence of the sum over all states  $|\psi\rangle$  in the first line above.

In order to set up the in-in perturbation theory we need to establish the propagator structure in the free theory. We encounter a  $2 \times 2$  propagator matrix  $D^{AB}(x, y)$  related to the doubled fields. It is most easily derived from the free-field generating functional  $W_0[J_1, J_2]$  in the operator representation (2.9) [13, 93] — see Appendix A for a derivation ( $A, B = 1, 2$ ):

$$\langle \phi_A(x) \phi_B(y) \rangle = \begin{pmatrix} \langle 0 | \mathcal{T} \phi(x) \phi(y) | 0 \rangle & \langle 0 | \phi(y) \phi(x) | 0 \rangle \\ \langle 0 | \phi(x) \phi(y) | 0 \rangle & \langle 0 | \mathcal{T}^* \phi(x) \phi(y) | 0 \rangle \end{pmatrix} = \begin{pmatrix} D_F(x, y) & D_-(x, y) \\ D_+(x, y) & D_D(x, y) \end{pmatrix}, \quad (2.12)$$

with the Feynman  $D_F(x, y)$  and Dyson (or anti-time-ordered)  $D_D(x, y)$  Green's function appearing on the diagonal. The off-diagonal entries are known as the Wightman Green's functions,  $D_+(x, y) = \langle 0 | \phi(x) \phi(y) | 0 \rangle = D_-(y, x)$ . Note that here  $|0\rangle$  is the Fock vacuum of the *free* theory which is stationary under time evolution.

We find it convenient to adopt the Keldysh basis [46] by introducing the sum and difference of the two fields and sources:

$$\begin{aligned} \phi_- &= \phi_1 - \phi_2, & \phi_+ &= \frac{1}{2}(\phi_1 + \phi_2), \\ J_- &= J_1 - J_2, & J_+ &= \frac{1}{2}(J_1 + J_2). \end{aligned} \quad (2.13)$$



The propagator matrix in the Keldysh basis then becomes ( $a, b = +, -$ ) [13]

$$\langle \phi_a(x) \phi_b(y) \rangle = \begin{pmatrix} \frac{1}{2} D_H(x, y) & D_{\text{ret}}(x, y) \\ -D_{\text{adv}}(x, y) & 0 \end{pmatrix}, \quad (2.14)$$

with the advanced  $D_{\text{adv}}(x, y)$  and retarded  $D_{\text{ret}}(x, y)$  Greens's functions as well as the symmetric Hadamard function  $D_H(x, y) = \langle 0 | \{ \phi(x), \phi(y) \} | 0 \rangle$ . In the Keldysh basis the generating functional of the interacting theory takes the form

$$e^{\frac{i}{\hbar} W[J_+, J_-]} \quad (2.15)$$

$$= \int \mathcal{D}[\phi_+, \phi_-] \exp \left\{ \frac{i}{\hbar} \left[ S[\phi_+ + \frac{1}{2} \phi_-] - S[\phi_+ - \frac{1}{2} \phi_-] + \int d^4x \left( J_+ \phi_- + J_- \phi_+ \right) \right] \right\}.$$

The true vacuum expectation value of the Heisenberg field operator may now be computed from the one-point function of  $\phi_+$  at vanishing sources  $J_{\pm}$  by

$$\langle \hat{\phi}_H(t, \mathbf{x}) \rangle_{\text{in-in}} = \langle \hat{\phi}_{H+}(t, \mathbf{x}) \rangle_{\text{in-in}} \Big|_{J_{\pm}=0} = \frac{\delta W[J_+, J_-]}{\delta J_-} \Big|_{J_{\pm}=0} \quad (2.16)$$

$$= \int \mathcal{D}[\phi_+, \phi_-] \phi_+(t, \mathbf{x}) \exp \left\{ \frac{i}{\hbar} \left[ S[\phi_+ + \frac{1}{2} \phi_-] - S[\phi_+ - \frac{1}{2} \phi_-] \right] \right\},$$

using  $\langle \phi_1 \rangle_{\text{in-in}}|_{J_i=0} = \langle \phi_2 \rangle_{\text{in-in}}|_{J_i=0}$  in the Schwinger basis. Importantly, the in-in effective action  $\Gamma[\langle \phi_{\pm} \rangle]$  is obtained as the Legendre transform of the generating functional

$$\Gamma[\langle \phi_+ \rangle, \langle \phi_- \rangle] = W[J_+, J_-] - \int d^4x \left( J_- \langle \phi_+ \rangle + J_+ \langle \phi_- \rangle \right). \quad (2.17)$$

Finally, at tree level the in-in effective action gives rise to the classical equations of motion that are solved by the expectation value (2.16):

$$0 = \frac{\delta \Gamma}{\delta \langle \phi_- \rangle} \Big|_{\langle \phi_- \rangle=0, \langle \phi_+ \rangle=\phi_{\text{class}}, J_{\pm}=0}. \quad (2.18)$$

Note that at tree level the  $\langle \phi_+ \phi_+ \rangle$  component  $D_H(x, y)$  of the Keldysh propagator matrix (2.14) does not contribute — in momentum space it is  $\tilde{D}_H(k) = \delta(k^2)$  and only has on-shell support — as we will show this in the next section. Hence, the tree-level or classical physics result can only depend on advanced and retarded propagators. This is the key relation to exploit for our purposes: applying the in-in formalism to the computation of the one-point functions  $\langle z_i^\mu \rangle$  and  $\langle h_{\mu\nu} \rangle$  of WQFT yields a PM perturbative, diagrammatic procedure to establish the solutions  $z_{\text{class}}(\tau)$  and  $h_{\text{class}}^{\mu\nu}(t, \mathbf{x})$  to the equations of motion of the classical two-body scattering problem.

### 2.3 In-in one-point functions in background field theory

Evaluating the in-in path integral can be quite laborious due to the need to establish “doubled” Feynman rules from eq. (2.15) — now adopting the Keldysh basis. These

involve vertices dressed with plus- and minus-labeled legs and novel symmetry factors (the tensorial structure of the vertices remains inert with respect to the standard in-out Feynman rules). As for the propagators, in momentum space the retarded and advanced propagators are

$$\begin{aligned}\tilde{D}_{\text{ret}}(k) &= \begin{array}{c} \bullet \longrightarrow \bullet \\ - \qquad \qquad + \end{array} = \frac{-i}{(k^0 + i0)^2 - \mathbf{k}^2}, \\ \tilde{D}_{\text{adv}}(k) &= \begin{array}{c} \bullet \longleftarrow \bullet \\ + \qquad \qquad - \end{array} = \frac{-i}{(k^0 - i0)^2 - \mathbf{k}^2},\end{aligned}\tag{2.19}$$

with the direction of the arrow above indicating the direction of causality flow —  $i0$  denotes a small *positive* imaginary part. However, for the special case of tree-level one-point functions in a background field theory the in-in diagrammatics are very simple: here we demonstrate that one needs only draw tree-level in-out graphs, but with retarded propagators replacing Feynman propagators.

Sticking to the scalar field example, the interaction vertices emerge from the in-in action (2.15). In perturbation theory the interacting part of the Lagrangian is polynomial in the fields. Hence, expanding the Lagrangian (2.15) gives rise to a series of vertices dressed with plus- and minus-labeled legs. Expanding  $S_{\text{in-in}}[\phi_-, \phi_+; Q] = S[\phi_+ + \frac{1}{2}\phi_-] - S[\phi_+ - \frac{1}{2}\phi_-]$  in the minus-labeled fields  $\phi_-$  it is obvious that only vertices with an *odd* number of minus legs will arise. At linear order in minus fields the vertex structure is particularly simple:

$$S_{\text{in-in,int}}[\phi_-, \phi_+; Q] = \phi_- \left( \frac{\delta S_{\text{int}}[\phi; Q]}{\delta \phi} \right)_{\phi \rightarrow \phi_+} + \mathcal{O}(\phi_-^3),\tag{2.20}$$

and importantly  $S_{\text{int}}[\phi; Q]$  is the original interacting piece of the (in-out) action (2.1). Hence, for the single-minus leg vertices we find precisely the same Feynman rules (including symmetry factors) as in the in-out formalism, with the distinction that these are extended by dressing each leg successively by a minus label and all others by a plus label.

Importantly, starting with the one-point vertices connected to the background  $Q$  the emitted graviton field always carries a minus label:

$$\begin{array}{c} \times \\ \downarrow \\ \phi_- \end{array}\tag{2.21}$$

where the cross symbolizes the background field  $Q$ . On the contrary, the outgoing leg relevant for the one-point functions  $\langle \phi_H \rangle$  is strictly plus labeled, c.f. (2.16). This leads to the following causality flow for a tree-level one-point function in the  $Q$

background:

$$\langle \phi(k) \rangle = \text{Diagram} \quad (2.22)$$

The grey shaded rectangle subsumes all tree-level interactions containing two-valent, three-valent and higher-point vertices that connect the  $n$  ingoing retarded propagators emerging from the background  $Q$  to the single outgoing leg.

The crucial insight is that at tree level only vertices with a *single minus leg* can contribute to these one-point functions. Any tree-level graph will have the topological structure of a rooted tree, i.e. take a form such as

$$\text{Diagram} \quad (2.23)$$

From this structure it is immediately clear that inserting a vertex with three (or more) minus-labeled (outgoing) legs in the shaded box inevitably leads to a loop-level graph, as we just have a single outgoing leg. So we learn that *at tree level only single-minus vertices may contribute* to the one-point functions. Similarly, the  $\langle \phi_+ \phi_+ \rangle$  Hadamard propagator cannot make an appearance, as connecting to plus labeled (ingoing) legs of a vertex inevitably yields a loop diagram as every vertex has at least one minus labeled leg. The consequence is that *exclusively retarded propagators* appear in the computation if one assigns a momentum flow according to causality from  $Q$  sources to the outgoing operator line. Therefore, in practical computations of one-point functions in a background field theory one may effectively forget about the in-in formalism altogether. One simply applies the usual (in-out) Feynman rules and uses retarded propagators everywhere, with the direction of causality always pointing towards the outgoing line.

In hindsight, this fact is not surprising. As we showed in eq. (2.18), it is a well-known fact that at tree level the path integral is dominated by solutions to the classical equations of motion of the theory (the saddle-point approximation). The sum of rooted tree diagrams is then simply a visual interpretation of a perturbative expansion of the classical solution in powers of the coupling constant. From a purely classical perspective, using retarded propagators is then necessary to ensure fixing of boundary conditions at past infinity.

## 2.4 In-in formalism for WQFT: observables

We now implement the in-in formalism for the WQFT. In the non-spinning case there are two key observables to be computed which we typically evaluate in momentum space: The impulse and the waveform. In the spinning case this is augmented by the spin-kick. For the worldline coordinate we expand  $x_i^\mu(\tau_i) = b_i^\mu + v_i^\mu \tau_i + z_i^\mu(\tau_i)$  with  $i = 1, 2$  denoting the two compact objects. In the in-in path integral we are led to double the fluctuation field  $z_i^\mu \rightarrow \{z_{i+}^\mu, z_{i-}^\mu\}$  but we do not double the background  $b_i^\mu + v_i^\mu \tau_i$ . This is justified, as in the end of the calculation the expectation value of the minus fields are set to zero, cp. (2.18). We proceed analogously in the spin case [49, 50], where we have the background field expansion  $\psi_i^\mu = \Psi_i^\mu + \psi_i^{\prime\mu}$ , and double according to  $\psi_i^{\prime\mu} \rightarrow \{\psi_{i+}^{\prime\mu}, \psi_{i-}^{\prime\mu}\}$  in the Keldysh basis. Finally, the graviton field is doubled according to  $h^{\mu\nu} \rightarrow \{h_+^{\mu\nu}, h_-^{\mu\nu}\}$ .

Let us now establish the Feynman rules for the in-in WQFT. As we argued in the last section if one is interested in tree-level one-point functions (as we are) we only need the retarded propagators. We then have for the graviton

$$\begin{array}{c} \mu\nu \rightarrow \rho\sigma \\ \bullet \text{---} \text{wavy} \text{---} \bullet \\ - \quad k \quad + \end{array} = i \frac{P_{\mu\nu;\rho\sigma}}{(k^0 + i0)^2 - \mathbf{k}^2}, \quad (2.24)$$

with  $P_{\mu\nu;\rho\sigma} := \eta_{\mu(\rho}\eta_{\sigma)\nu} - \frac{1}{D-2}\eta_{\mu\nu}\eta_{\rho\sigma}$ . The retarded worldline propagators for the fluctuations  $z_i^\mu(\omega)$  and anti-commuting vectors  $\psi_i^{\prime\mu}(\omega)$  are respectively

$$\begin{array}{c} \mu \rightarrow \nu \\ \bullet \text{---} \text{---} \bullet \\ - \quad \omega \quad + \end{array} = -i \frac{\eta^{\mu\nu}}{m_i(\omega + i0)^2}, \quad \begin{array}{c} \mu \rightarrow \nu \\ \bullet \text{---} \text{---} \bullet \\ - \quad \omega \quad + \end{array} = -i \frac{\eta^{\mu\nu}}{m_i(\omega + i0)}. \quad (2.25)$$

Note that now the direction of the arrow above the propagators indicates the causality flow. The retarded propagators were already used in [47–51].

For the in-in WQFT vertices at linear order in minus fields the vertex structure is particularly simple — generalizing the scalar field discussion of eq. (2.20):

$$\begin{aligned} S_{\text{in-in, int}}^{\text{WQFT}} \Big|_{\text{lin-}} &= h_-^{\mu\nu} \left( \frac{\delta S_{\text{int}}^{\text{WQFT}}[h, z, \psi']}{\delta h^{\mu\nu}} \right)_+ + \sum_{i=1}^2 z_{i-}^\mu \left( \frac{\delta S_{\text{int}}^{\text{WQFT}}[h, z, \psi']}{\delta z_i^\mu} \right)_+ \\ &+ \sum_{i=1}^2 \psi_{i-}^{\prime\mu} \left( \frac{\delta S_{\text{int}}^{\text{WQFT}}[h, z, \psi']}{\delta \psi_i^{\prime\mu}} \right)_+. \end{aligned} \quad (2.26)$$

We find precisely the same Feynman rules (including symmetry factors) as in the in-out formalism, with the distinction that these are extended by dressing each leg successively by a minus label and all others by a plus label. Importantly, starting with the one-point functions connected to the background trajectories the connecting graviton field always carries a minus label:

$$\begin{array}{c} - \\ \text{---} \text{---} \text{---} \text{---} \text{---} \\ \bullet \\ \text{---} \text{---} \text{---} \text{---} \text{---} \\ \downarrow \\ h_{\mu\nu}(k) \end{array}, \quad (2.27)$$

while the tensorial structure remains as before [47–51]. Again, the outgoing leg relevant for the one-point functions  $\langle h_+^{\mu\nu}(k) \rangle$ ,  $\langle z_{i+}^\mu(\omega) \rangle$  or  $\langle \psi'_{i+}{}^\mu(\omega) \rangle$  is strictly plus by virtue of (2.16).

This leads to the following causality structure for the WQFT in the in-in formalism: for the graviton emission

$$\langle h^{\mu\nu}(k) \rangle = \text{Diagram} \quad (2.28)$$

as well as for the worldline one-point functions

$$\langle z_1^\mu(\omega) \rangle = \text{Diagram} \quad (2.29)$$

$$\langle \psi'_1{}^\mu(\omega) \rangle = \text{Diagram} \quad (2.30)$$

As we learnt in the previous section, inside the grey shaded rectangle we should only insert single-minus-leg vertices. Ironically we may then effectively forget about the in-in formalism altogether: simply apply the standard (in-out) Feynman rules, assign momenta according to the causality flow (from one-point worldline vertices to the outgoing line) and use retarded propagators everywhere. This is what was done (and its correctness implicitly assumed) in our previous works [47–51]. Here we have given a derivation of this property.

## 2.5 In-in formalism for WQFT: free energy

The eikonal phase in the scattering amplitudes approach to classical gravitational scattering [68, 79, 81, 95] plays the role of a generating functional for the observables (impulse and spin kick). The eikonal phase generalizes in WQFT to the free energy  $\chi(b^\mu, v_i^\mu, \Psi_i^\mu)$ , which is a function of the background parameters. In refs. [47, 50] it was shown to yield the impulse and spin kick by differentiation with respect to  $b^\mu$  and  $\Psi_i^\mu$  respectively. However, in the presence of radiation-reaction we need

to generalize this construction to the in-in formalism. We therefore now modify the in-in prescription for the background configurations: we introduce a plus- and minus-labeled background, i.e. we expand  $x_{i\pm}^\mu(\tau_i) = b_{i\pm}^\mu + v_{i\pm}^\mu \tau_i + z_{i\pm}^\mu(\tau_i)$  and  $\psi_{i\pm}^\mu(\tau_i) = \Psi_{i\pm}^\mu + \psi'_{i\pm}^\mu(\tau_i)$ . Importantly, the in-in free energy or zero-point function  $\chi_{\text{in-in}}$  then needs to be evaluated only to *linear* order in the minus background fields  $b_{i-}, v_{i-}$  and  $\Psi_{i-}$ . This is so as the observables are derived from the in-in free energy via

$$\Delta p_{\mu,i} = -\frac{\partial \chi_{\text{in-in}}}{\partial b_{i-}^\mu} \Big|_{b_- = v_- = \Psi_- = 0}, \quad im_i \Delta \psi_{\mu,i} = \frac{\partial \chi_{\text{in-in}}}{\partial \bar{\Psi}_{i-}^\mu} \Big|_{b_- = v_- = \Psi_- = 0}, \quad (2.31)$$

identifying the plus-labeled background parameters with the physical ones:  $b_{i+}^\mu = b_i^\mu$ ,  $v_{i+}^\mu = v_i^\mu$  and  $\Psi_{i+}^\mu = \Psi_i^\mu$ .

In summary we find the following prescription: write down all zero-point diagrams with the in-out Feynman rules and successively assign to every vertex on the worldlines a minus-labeled background. This single ‘‘hot’’ worldline vertex in a diagram then acts as a ‘‘sink’’ for the causality flow, meaning that all propagators directed towards it are taken to be retarded. This prescription manifestly guarantees the differential relations above. Yet, effectively this prescription is no more efficient than computing the observables directly as discussed above, as the so-defined in-in free energy takes the form

$$\chi_{\text{in-in}} = \sum_{i=1}^2 -b_{i-}^\mu \Delta p_{\mu,i} + im_i \bar{\Psi}_{i-}^\mu \Delta \psi_{\mu,i} + \dots, \quad (2.32)$$

where the dots refer to terms quadratic in the minus background or linear in  $v_{i-}$ . Thus, there is no gain in efficiency in evaluating the in-in free energy to the direct computation of the observables: deflection and spin kick.

### 3 Retarded integrals

Having shown that complete WQFT observables naturally involve retarded propagators we now study a family of Feynman integrals involving these instead of the usual time-symmetric Feynman type. We focus on the following class of integrals relevant for deriving classical observables in the gravitational scattering of two comparable-mass bodies at 3PM order:

$$I_{n_1, n_2, \dots, n_7}^{(\sigma_1; \sigma_2; \sigma_3)} := \int_{\ell_1, \ell_2} \frac{\bar{\delta}(\ell_1 \cdot v_2) \bar{\delta}(\ell_2 \cdot v_1)}{D_1^{n_1} D_2^{n_2} \dots D_7^{n_7}}, \quad (3.1)$$

$$D_1 = \ell_1 \cdot v_1 + \sigma_1 i0, \quad D_2 = \ell_2 \cdot v_2 + \sigma_2 i0, \quad D_3 = (\ell_1 + \ell_2 - q)^2 + \sigma_3 \text{sgn}(\ell_1^0 + \ell_2^0 - q^0) i0, \\ D_4 = \ell_1^2, \quad D_5 = \ell_2^2, \quad D_6 = (\ell_1 - q)^2, \quad D_7 = (\ell_2 - q)^2,$$

where  $\bar{\delta}(\omega) := 2\pi\delta(\omega)$ ,  $\int_k := \int \frac{d^D k}{(2\pi)^D}$  in  $D = 4 - 2\epsilon$  dimensions and  $\sigma_i = \pm 1$  determine the  $i0$  prescription. The two velocities  $v_i^\mu$  are time-like vectors satisfying  $v_i^2 = 1$ ; the

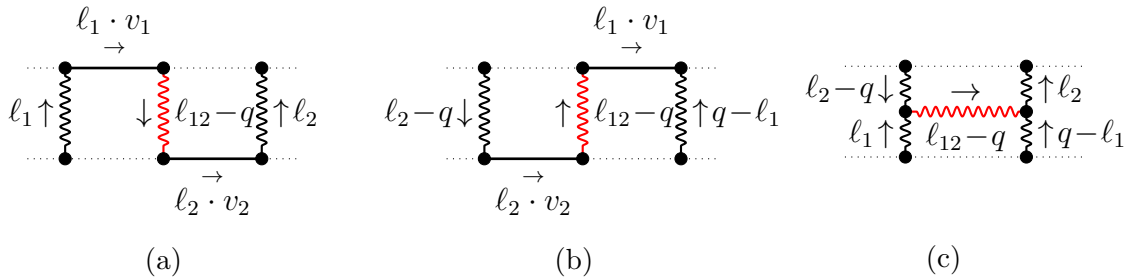


**Figure 1:** A selection of three diagrams involved in the integral family  $I_{n_1, n_2, \dots, n_7}^{(\sigma_1; \sigma_2; \sigma_3)}$  (3.1), with  $\ell_{12}^\mu = \ell_1^\mu + \ell_2^\mu$ . Wiggly lines propagating in the bulk represent massless propagators  $(\ell^2 \pm \text{sgn}(\ell^0)i0)^{-n}$ ; solid lines propagating on the worldlines (dotted) represent linear propagators  $(\omega \pm i0)^{-n}$ . The propagator highlighted in red corresponds with  $D_3$  (3.1), and is the only *active* bulk propagator — i.e. the only one with the ability to go on shell.

exchanged momentum  $q^\mu$  is a space-like vector satisfying  $q \cdot v_i = 0$ . In general, the integrals are functions only of  $\gamma = v_1 \cdot v_2$  and  $|q| := \sqrt{-q \cdot q}$ ; as the latter dependence is trivially fixed on dimensional grounds we can safely set  $|q| = 1$ . A selection of three WQFT Feynman graphs giving rise to these integrals is shown in Fig. 1.

We begin with some general remarks. The two linearized propagators  $D_1$  and  $D_2$  are associated with deflection modes propagating on the worldlines; the quadratic propagators  $D_3$ – $D_7$  with massless particles propagating in the bulk. Of these five propagators only the first,  $D_3$ , can go on-shell over the constrained (by the  $\delta$ -functions) domain of integration; for the others  $D_i \neq 0$  generically as we may choose a frame that ensures these propagators become Euclidean, i.e.  $\ell_i^2 = -\ell_i^2$ . We therefore refer to  $D_3$  as an *active* propagator, and track  $i0$  prescriptions only on  $D_{1,2,3}$ . As we shall see, the velocity scaling of  $k^\mu := \ell_1^\mu + \ell_2^\mu - q^\mu$  in  $D_3$  determines our region of integration (potential or radiation) in the static limit  $v \rightarrow 0$ .

Feynman integrals with retarded propagators are always purely real or imaginary (pseudoreal). In the current context this is necessarily true, as we will construct real physical observables as linear combinations of these integrals with (pseudo)real coefficients. We can also show it directly by taking the complex conjugate, which sends  $i0 \rightarrow -i0$  everywhere:

$$\begin{aligned}
& I_{n_1, n_2, \dots, n_7}^{(\sigma_1; \sigma_2; \sigma_3)*} \\
&= \int_{\ell_1, \ell_2} \frac{\delta(\ell_1 \cdot v_2) \delta(\ell_2 \cdot v_1)}{(\ell_1 \cdot v_1 - \sigma_1 i0)^{n_1} (\ell_2 \cdot v_2 - \sigma_2 i0)^{n_2} ((\ell_1 + \ell_2 - q)^2 - \sigma_3 \text{sgn}(\ell_1^0 + \ell_2^0 - q^0) i0)^{n_3} \dots} \\
&= \int_{\ell_1, \ell_2} \frac{\delta(\ell_1 \cdot v_2) \delta(\ell_2 \cdot v_1)}{(-\ell_1 \cdot v_1 - \sigma_1 i0)^{n_1} (-\ell_2 \cdot v_2 - \sigma_2 i0)^{n_2} ((\ell_1 + \ell_2 - q)^2 + \sigma_3 \text{sgn}(\ell_1^0 + \ell_2^0 - q^0) i0)^{n_3} \dots} \\
&= (-1)^{n_1 + n_2} I_{n_1, n_2, \dots, n_7}^{(\sigma_1; \sigma_2; \sigma_3)}. \tag{3.2}
\end{aligned}$$

In the second step we have replaced  $\ell_i^\mu \rightarrow -\ell_i^\mu$ ,  $q^\mu \rightarrow -q^\mu$ .<sup>1</sup> We relied here on

<sup>1</sup>The latter is possible as  $I_{n_1, n_2, \dots, n_7}^{(\sigma_1; \sigma_2; \sigma_3)}$  only depends on  $q^\mu$  via  $|q|$ .

the velocities  $v_i^\mu$  being real, time-like vectors: so this argument applies strictly in the physical regime  $1 < \gamma < \infty$ . We see a clear separation into two sub-families of integrals: those with even or odd values of  $n_1 + n_2$ , which are purely real or imaginary.

There is also a close relationship to integrals involving the Feynman  $i0$  prescription. We remind ourselves that Feynman and retarded propagators may be decomposed according to<sup>2</sup>

$$\frac{1}{k^2 + i0} = \mathcal{P} \frac{1}{k^2} - i\pi \delta(k^2), \quad (3.3a)$$

$$\frac{1}{k^2 + \sigma \operatorname{sgn}(k^0) i0} = \mathcal{P} \frac{1}{k^2} - i\pi \sigma \operatorname{sgn}(k^0) \delta(k^2). \quad (3.3b)$$

Here  $\mathcal{P}$  refers to a principal value prescription. Specializing to  $n_1 = n_2 = 0$  (no worldline propagators) and  $n_3 = 1$ :

$$I_{0,0,1,n_4,n_5,n_6,n_7}^{(\sigma_1;\sigma_2;\sigma_3)} = \int_{\ell_1,\ell_2} \frac{\delta(\ell_1 \cdot v_2) \delta(\ell_2 \cdot v_1)}{(\ell_1^2)^{n_4} (\ell_2^2)^{n_5} ((\ell_1 - q)^2)^{n_6} ((\ell_2 - q)^2)^{n_7}} \times \quad (3.4)$$

$$\left( \mathcal{P} \frac{1}{(\ell_1 + \ell_2 - q)^2} - i\pi \sigma_3 \operatorname{sgn}(\ell_1^0 + \ell_2^0 - q^0) \delta((\ell_1 + \ell_2 - q)^2) \right).$$

The on-shell contribution proportional to  $\sigma_3$  vanishes by symmetry. The entire integral is therefore given by its principal value part, and thus the real part of the same integral where a Feynman  $i0$  prescription is used instead.

To obtain explicit expressions for these integrals we take a well-studied approach [68, 80, 89, 96, 97]: seek linear identities between the integrals arising from symmetries and integration-by-parts (IBP) relations, and reduce to a basis of masters [98, 99]. Expressions are then recovered by solving differential equations (DEs) in  $\gamma$  [100]. Finally, constants of integration are fixed by comparison with the static limit  $v \rightarrow 0$ , where  $v$  is the relative velocity and  $\gamma = (1 - v^2)^{-1/2}$  using the method of regions [101]. The only aspects specifically affected by the retarded  $i0$  prescription are the symmetry relations and the fixing of boundary conditions in the static limit.

### 3.1 Linear identities

We begin with the symmetry relations. Naively there are eight families of integrals, corresponding to the possible sign choices on  $\sigma_i$ . However, the integrals satisfy

$$I_{n_1,n_2,n_3,n_4,n_5,n_6,n_7}^{(\sigma_1;\sigma_2;\sigma_3)} = I_{n_1,n_2,n_3,n_6,n_7,n_4,n_5}^{(\sigma_1;\sigma_2;\sigma_3)} \quad (\text{shift } \ell_i^\mu \rightarrow \ell_i^\mu + q^\mu), \quad (3.5a)$$

$$I_{n_1,n_2,n_3,n_4,n_5,n_6,n_7}^{(\sigma_1;\sigma_2;\sigma_3)} = (-1)^{n_1+n_2} I_{n_1,n_2,n_3,n_4,n_5,n_6,n_7}^{(-\sigma_1;-\sigma_2;-\sigma_3)} \quad (\text{flip } \ell_i^\mu \rightarrow -\ell_i^\mu, q^\mu \rightarrow -q^\mu), \quad (3.5b)$$

$$I_{n_1,n_2,n_3,n_4,n_5,n_6,n_7}^{(\sigma_1;\sigma_2;\sigma_3)} = I_{n_2,n_1,n_3,n_5,n_4,n_7,n_6}^{(\sigma_2;\sigma_1;\sigma_3)} \quad (\text{exchange } \ell_1^\mu \leftrightarrow \ell_2^\mu, v_1^\mu \leftrightarrow v_2^\mu). \quad (3.5c)$$

---

<sup>2</sup>One should be careful applying such distributional identities when products of propagators are involved; however, in the present context there is no such issue.



Using the second two relations (3.5b) and (3.5c) we are left with three independent families, which we choose as

$$I_{n_1, n_2, \dots, n_7} = I_{n_1, n_2, \dots, n_7}^{(+; +; +)}, \quad I'_{n_1, n_2, \dots, n_7} = I_{n_1, n_2, \dots, n_7}^{(-; -; +)}, \quad I''_{n_1, n_2, \dots, n_7} = I_{n_1, n_2, \dots, n_7}^{(+; -; +)}. \quad (3.6)$$

When one of the propagators  $D_1$ – $D_3$  is raised to a zero or negative power, i.e. that propagator is now a numerator, then there is overlap between the different families:

$$I_{n_1, n_2, \dots, n_7}^{(+; \sigma_2; \sigma_3)} = I_{n_1, n_2, \dots, n_7}^{(-; \sigma_2; \sigma_3)}, \quad n_1 \leq 0, \quad (3.7a)$$

$$I_{n_1, n_2, \dots, n_7}^{(\sigma_1; +; \sigma_3)} = I_{n_1, n_2, \dots, n_7}^{(\sigma_1; -; \sigma_3)}, \quad n_2 \leq 0, \quad (3.7b)$$

$$I_{n_1, n_2, \dots, n_7}^{(\sigma_1; \sigma_2; +)} = I_{n_1, n_2, \dots, n_7}^{(\sigma_1; \sigma_2; -)}, \quad n_3 \leq 0. \quad (3.7c)$$

In these cases the  $i0$  prescription is irrelevant.

The other identities are IBP relations, conveniently generated using on-the-market tools including FIRE [102], LiteRed [103, 104] and KIRA [105, 106]. As these are fairly conventional we will not go into detail regarding our use of them here; the only subtlety is our handling of the  $\delta(\ell_1 \cdot v_2)$  and  $\delta(\ell_2 \cdot v_1)$  present in eq. (3.1). Following refs. [80, 96], when generating IBPs we generalize them to include derivatives:

$$\frac{\delta^{(n)}(\omega)}{(-1)^n n!} = \frac{i}{(\omega + i0)^{n+1}} - \frac{i}{(\omega - i0)^{n+1}}. \quad (3.8)$$

Four-dimensional Lorentz covariance is maintained by treating these  $\delta$ -functions as cut propagators. From this perspective our integrals thus have nine propagators instead of seven, but in general we always choose masters adhering to the schematic form (3.1).

### 3.2 Canonical bases

While in principle any linearly independent set of integrals would suffice as a set of master integrals, it is convenient to choose a so-called canonical basis [100]. A suitable basis of real master integrals (also used in ref. [97],  $\epsilon = 2 - \frac{D}{2}$ ) is

$$\mathcal{I}_1 = 2\epsilon^2 I_{0,0,0,1,1,1,1}, \quad (3.9a)$$

$$\mathcal{I}_2 = 2\epsilon^2 \sqrt{\gamma^2 - 1} I_{0,0,1,0,0,1,1}, \quad (3.9b)$$

$$\mathcal{I}_3 = 2\epsilon \sqrt{\gamma^2 - 1} I_{0,0,2,0,0,1,1}, \quad (3.9c)$$

$$\mathcal{I}_4 = -4I_{-1,-1,3,0,0,1,1} + (1 + 2\epsilon)\gamma I_{0,0,2,0,0,1,1}, \quad (3.9d)$$

$$\mathcal{I}_5 = \frac{2(4\epsilon - 1)(2\epsilon - 1)}{\sqrt{\gamma^2 - 1}} I_{0,0,1,0,1,0,1}, \quad (3.9e)$$

$$\mathcal{I}_6 = 2\epsilon^2 \sqrt{\gamma^2 - 1} I_{0,0,1,1,1,1,1}, \quad (3.9f)$$

$$\mathcal{I}_7 = -8\epsilon^2 I_{-1,-1,1,1,1,1,1} + 4\epsilon^2 \gamma I_{0,0,0,1,1,1,1}, \quad (3.9g)$$

$$\mathcal{I}_8 = -\epsilon^2 (\gamma^2 - 1) I_{1,1,1,0,0,1,1}, \quad (3.9h)$$

with  $\mathcal{I}'_i$  and  $\mathcal{I}''_i$  similarly defined in terms of  $I'_{n_1, n_2, \dots, n_7}$  and  $I''_{n_1, n_2, \dots, n_7}$  (3.6). Introducing  $x = \gamma - \sqrt{\gamma^2 - 1}$ , so that  $0 < x < 1$  in the physical region, the defining property of this canonical basis is that the resulting system of DEs takes an  $\epsilon$ -factorized form:

$$\frac{d\vec{\mathcal{I}}}{dx} = \epsilon \left( \frac{A}{x} + \frac{B_+}{1+x} - \frac{B_-}{1-x} \right) \vec{\mathcal{I}}, \quad (3.10)$$

which one observes by explicitly differentiating the master integrals (3.9) and reducing the resulting integrals via IBPs to the same basis. The set of poles  $\{x, 1+x, 1-x\}$  is the symbol alphabet; the constant matrices are

$$A = \begin{pmatrix} 0 & 0 & 0 & 0 & 0 & 0 & 0 & 0 \\ 0 & -6 & 0 & -1 & 0 & 0 & 0 & 0 \\ 0 & 0 & 2 & -2 & 0 & 0 & 0 & 0 \\ 0 & 12 & 2 & 0 & 0 & 0 & 0 & 0 \\ 0 & 0 & 0 & 0 & 2 & 0 & 0 & 0 \\ 0 & 0 & 4 & 2 & 4 & 2 & -2 & 0 \\ 0 & 12 & 8 & 0 & 8 & 2 & -2 & 0 \\ 0 & 0 & -1 & 0 & 0 & 0 & 0 & 0 \end{pmatrix}, \quad B_{\pm} = \begin{pmatrix} 0 & 0 & 0 & 0 & 0 & 0 & 0 & 0 \\ 0 & 6 & 0 & 0 & 0 & 0 & 0 & 0 \\ 0 & 0 & -2 & 0 & 0 & 0 & 0 & 0 \\ 0 & 0 & 0 & 0 & 0 & 0 & 0 & 0 \\ 0 & 0 & 0 & 0 & -2 & 0 & 0 & 0 \\ 0 & 0 & -4 & 0 & -4 & -2 & 0 & 0 \\ \pm 4 & 0 & 0 & 0 & 0 & 0 & 2 & 0 \\ 0 & 0 & 0 & 0 & 0 & 0 & 0 & 0 \end{pmatrix}, \quad (3.11)$$

and for the  $\vec{\mathcal{I}}'$ ,  $\vec{\mathcal{I}}''$  integrals we have  $A = A' = A''$ ,  $B_{\pm} = B'_{\pm} = B''_{\pm}$ . This  $\epsilon$ -factorized form of the DEs is solved as a series expansion in  $\epsilon$ :

$$\vec{\mathcal{I}} = \vec{\mathcal{I}}^{(0)} + \epsilon \vec{\mathcal{I}}^{(1)} + \mathcal{O}(\epsilon^2), \quad (3.12)$$

with solution

$$\vec{\mathcal{I}}^{(0)} = \vec{c}^{(0)}, \quad \vec{\mathcal{I}}^{(1)} = (A \log(x) + B_+ \log(1+x) - B_- \log(1-x)) \vec{\mathcal{I}}^{(0)} + \vec{c}^{(1)}. \quad (3.13)$$

The overlap relations (3.7) also tell us that

$$\mathcal{I}_i = \mathcal{I}'_i = \mathcal{I}''_i, \quad 1 \leq i \leq 7, \quad (3.14)$$

while  $\mathcal{I}_8$ ,  $\mathcal{I}'_8$  and  $\mathcal{I}''_8$  each have separate expressions. The only remaining subtlety is fixing the constants of integration  $\vec{c}^{(i)}$ , a point to which we will return in section 3.3.

A canonical basis for the purely imaginary integrals is

$$\mathcal{I}_9 = -2\epsilon \sqrt{\gamma^2 - 1} I_{1,0,1,0,1,0,1}, \quad (3.15a)$$

$$\mathcal{I}_{10} = -2\epsilon \sqrt{\gamma^2 - 1} I_{1,0,1,1,1,0,0}, \quad (3.15b)$$

$$\mathcal{I}_{11} = \frac{1-2\epsilon}{3} I_{1,0,1,1,0,1,0}, \quad (3.15c)$$

$$\mathcal{I}_{12} = I_{-1,0,2,0,0,1,1}, \quad (3.15d)$$

$$\mathcal{I}_{13} = -\epsilon I_{-1,0,1,1,1,1,1}. \quad (3.15e)$$

These five integrals also obey DEs of the form (3.10) but with  $5 \times 5$  matrices

$$A = \begin{pmatrix} 0 & 0 & 6 & 0 & 0 \\ 0 & 0 & 0 & -4 & 0 \\ 0 & 0 & 2 & 0 & 0 \\ 0 & 0 & 0 & -2 & 0 \\ 0 & 0 & 0 & -2 & 0 \end{pmatrix}, \quad B_+ = \begin{pmatrix} 0 & 0 & 0 & 0 & 0 \\ 0 & 0 & 0 & 0 & 0 \\ 0 & 0 & -2 & 0 & 0 \\ 0 & 0 & 0 & 6 & 0 \\ 0 & 0 & -6 & 0 & 2 \end{pmatrix}, \quad B_- = \begin{pmatrix} 0 & 0 & 0 & 0 & 0 \\ 0 & 0 & 0 & 0 & 0 \\ 0 & 0 & -2 & 0 & 0 \\ 0 & 0 & 0 & -2 & 0 \\ 0 & 0 & 6 & 4 & -2 \end{pmatrix}, \quad (3.16)$$

and  $A = A'$ ,  $B_\pm = B'_\pm$ . Similar expressions for  $\mathcal{I}'_i$  and  $\mathcal{I}''_i$  are again defined in terms of  $I'_{n_1, n_2, \dots, n_7}$  and  $I''_{n_1, n_2, \dots, n_7}$ ; in the latter case we require two additional masters

$$\mathcal{I}''_{14} = -2\epsilon\sqrt{\gamma^2 - 1}I_{0,1,1,1,0,1,0}^{(+;-;+)}, \quad (3.17a)$$

$$\mathcal{I}''_{15} = -2\epsilon\sqrt{\gamma^2 - 1}I_{0,1,1,1,1,0,0}^{(+;-;+)}, \quad (3.17b)$$

in order to have a complete basis. So in this case the DEs involve  $7 \times 7$  matrices. Fortunately, all seven of these integrals are given by the overlap relations (3.7):

$$\mathcal{I}''_i = \mathcal{I}_i, \quad 9 \leq i \leq 13, \quad (3.18a)$$

$$\mathcal{I}''_{14} = \mathcal{I}'_9, \quad \mathcal{I}''_{15} = \mathcal{I}'_{10}. \quad (3.18b)$$

We therefore focus on the  $\mathcal{I}_i$  and  $\mathcal{I}'_i$  families.

### 3.3 Method of regions

Our strategy for fixing boundary conditions on the integrals is to evaluate them to leading order in the static limit where  $v \rightarrow 0$ . However, this expansion requires caution as the two limits  $\epsilon \rightarrow 0$  and  $v \rightarrow 0$  do not generally commute [97, 107]. In order to expand the integrand in  $v \rightarrow 0$  before integration we use the *method of regions* [70, 80, 108, 109]. Here, one identifies all singular regions in the static limit and writes the full integral as a sum of contributions from each region [101]. Each of these contributions satisfy the same differential equations but behave differently in the static limit, which leads to different boundary conditions.

Regions in the static limit are characterized by velocity scalings of the loop momenta, with their time-like and spatial components scaling as

$$\ell_i^{\text{pot}} = (\ell_i^0, \boldsymbol{\ell}_i) \sim (v, 1), \quad (3.19a)$$

$$\ell_i^{\text{rad}} = (\ell_i^0, \boldsymbol{\ell}_i) \sim (v, v). \quad (3.19b)$$

These we refer to these as potential and radiative momenta: only radiative momenta can go on-shell,  $\ell_i^2 = 0$ . In the present context, we note that only the momentum  $k^\mu = \ell_1^\mu + \ell_2^\mu - q^\mu$ , carried by the active  $D_3$  propagator (3.1), may be radiative; for all other internal momenta the potential scaling (3.19a) is mandated by the presence of

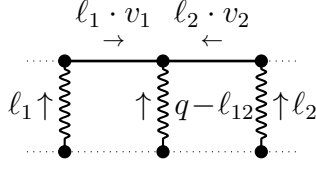


**Figure 2:** An example of a diagram contributing to the test-body integral family  $J_{n_1, n_2, \dots, n_7}^{(\sigma_1; \sigma_2)}$  (3.22), in which none of the massless lines can go on-shell.

$\delta(\ell_i \cdot v_j)$ . Thus, in the static limit the behavior of  $D_3$  characterizes the entire integral, splitting it into a sum of two regions:

$$I_{n_1, n_2, \dots, n_7}^{(\sigma_1; \sigma_2; \sigma_3)} = I_{n_1, n_2, \dots, n_7}^{(\sigma_1; \sigma_2; \sigma_3)\text{pot}} + I_{n_1, n_2, \dots, n_7}^{(\sigma_1; \sigma_2; \sigma_3)\text{rad}}, \quad (3.20)$$

which we again refer to as potential and radiation. In these two regions the integrand may be expanded in  $v$  assuming the momentum scalings (3.19), and boundary conditions are fixed by matching to the leading-order term in this expansion. The resulting integrals are simpler as their dependence on  $\gamma = (1 - v^2)^{-1/2}$  is trivialized.

Let us first analyze the potential region (also discussed in ref. [51]). Here all internal momenta live in the potential region (3.19a), so it makes no difference whether the  $D_3$  propagator is advanced or retarded. In the static limit to leading order in  $v$

$$I_{n_1, n_2, \dots, n_7}^{(\sigma_1; \sigma_2; \sigma_3)\text{pot}} = (-1)^{n_1} J_{n_1, n_2, \dots, n_7}^{(-\sigma_1; \sigma_2)} + \mathcal{O}(v^{2-n_1-n_2}), \quad (3.21)$$

where the integrals  $J_{n_1, n_2, \dots, n_7}^{(\sigma_1; \sigma_2)} \sim \mathcal{O}(v^{-n_1-n_2})$  are given by

$$J_{n_1, n_2, \dots, n_7}^{(\sigma_1; \sigma_2)} := \int_{\ell_1, \ell_2} \frac{\delta(\ell_1 \cdot v_2) \delta(\ell_2 \cdot v_1)}{D_1^{n_1} D_2^{n_2} \dots D_7^{n_7}}, \quad (3.22)$$

$$D_1 = \ell_1 \cdot v_1 + \sigma_1 i 0, \quad D_2 = \ell_2 \cdot v_1 + \sigma_2 i 0, \quad D_3 = (\ell_1 + \ell_2 - q)^2,$$

$$D_4 = \ell_1^2, \quad D_5 = \ell_2^2, \quad D_6 = (\ell_1 - q)^2, \quad D_7 = (\ell_2 - q)^2.$$

This integral family is familiar: in ref. [51] integrals of this kind were relevant for computing observables in the probe limit  $m_1 \ll m_2$ . With respect to IBP and symmetry relations there are three master integrals:

$$J_{0,0,1,1,1,0,0}^{(+; \pm)} = -(4\pi)^{-3+2\epsilon} \frac{\Gamma^3(\frac{1}{2} - \epsilon) \Gamma(2\epsilon)}{\Gamma(\frac{3}{2} - 3\epsilon)}, \quad (3.23a)$$

$$J_{1,0,1,1,1,0,0}^{(+; \pm)} = (4\pi)^{-\frac{5}{2}+2\epsilon} \frac{i}{2\sqrt{\gamma^2 - 1}} \frac{\Gamma(\frac{1}{2} - 2\epsilon) \Gamma^2(\frac{1}{2} - \epsilon) \Gamma(-\epsilon) \Gamma(\frac{1}{2} + 2\epsilon)}{\Gamma(\frac{1}{2} - 3\epsilon) \Gamma(1 - 2\epsilon)}, \quad (3.23b)$$

$$J_{1,1,1,1,1,0,0}^{(+; +)} = -2J_{1,1,1,1,1,0,0}^{(+; -)} = (4\pi)^{-2+2\epsilon} \frac{\Gamma^3(-\epsilon) \Gamma(1 + 2\epsilon)}{3(\gamma^2 - 1) \Gamma(-3\epsilon)}, \quad (3.23c)$$

and as promised the dependence on  $\gamma$  and  $\epsilon$  factorizes. An example of a WQFT diagram giving rise to such integrals is displayed in Fig. 2. As none of the internal

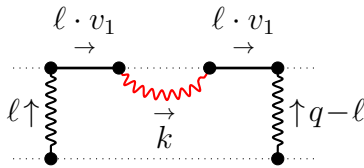


**Figure 3:** A schematic representation of the “mushroom” integral family  $K_{n_1, n_2, \dots, n_5}^{(\sigma_1; \sigma_2; \sigma_3)}$ , in which the propagator carrying momentum  $k^\mu$  is radiative (red line).

momenta can go on-shell this integral family consists only of rational functions of the dimension  $D = 4 - 2\epsilon$ .

Next we turn to the region where  $k^\mu = \ell_1^\mu + \ell_2^\mu - q^\mu$  is radiative and  $\ell^\mu = \ell_1^\mu$  lives in the potential region. We find that

$$I_{n_1, n_2, \dots, n_7}^{(\sigma_1; \sigma_2; \sigma_3)\text{rad}} = K_{n_1, n_2, n_3, n_4 + n_7, n_5 + n_6}^{(\sigma_1; \sigma_2; \sigma_3)} + \mathcal{O}(v^{D+1-n_1-n_2-2n_3}), \quad (3.24)$$

where the new integral family  $K_{n_1, n_2, \dots, n_7}^{(\sigma_1; \sigma_2; \sigma_3)} \sim \mathcal{O}(v^{D-1-n_1-n_2-2n_3})$  is defined as

$$K_{n_1, n_2, \dots, n_5}^{(\sigma_1; \sigma_2; \sigma_3)} := \int_{\ell, k} \frac{\delta((k - \ell) \cdot v_1) \delta(\ell \cdot v_2)}{(\ell \cdot v_1 + \sigma_1 i 0)^{n_1} (\ell \cdot v_1 + \sigma_2 i 0)^{n_2} (k^2 + \sigma_3 \text{sgn}(k^0) i 0)^{n_3} (\ell^2)^{n_4} ((\ell - q)^2)^{n_5}}. \quad (3.25)$$

These integrals (sometimes called “mushrooms”) describe self-interaction where a worldline emits and absorbs the same graviton. A schematic representation of these integrals is given in Fig. 3. It is tempting to assume that these integrals form a subset of the  $I_{n_1, n_2, \dots, n_7}^{(\sigma_1; \sigma_2; \sigma_3)}$  family (3.1); however, this is only true when  $\sigma_1 = \sigma_2$ .

The split into regions (3.20) can also be understood diagrammatically. In Fig. 4 we draw the two diagrams corresponding with the  $J_{n_1, n_2, \dots, n_7}^{(\sigma_1; \sigma_2)}$  and  $K_{n_1, n_2, \dots, n_5}^{(\sigma_1; \sigma_2; \sigma_3)}$  integrals identified in the static limit. The procedure can be interpreted as moving one of the worldline propagators between the two worldlines, using the fact that  $v_1^\mu = v_2^\mu$  to leading order in the static limit. The only difficulty is handling the “active” propagator which gives rise to two different choices: it can either connect the two worldlines, or the same worldline twice. These are precisely the potential and radiation regions.

### 3.4 Mushroom integrals

We analyze the mushroom integrals  $K_{n_1, n_2, \dots, n_5}^{(\sigma_1; \sigma_2; \sigma_3)}$  (3.25) in more detail, as these are sensitive to the  $i0$  prescription of the active bulk propagator. They are nested single-scale one-loop integrals. Without loss of generality we choose  $\sigma_1 = 1$ ,  $\sigma_2 = -1$  and  $\sigma_3 = 1$ , so that  $n_1$  and  $n_2$  count powers of retarded and advanced worldline propagators respectively, while  $n_3$  counts powers of the retarded bulk propagator.

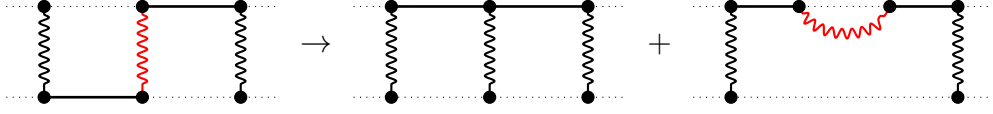


**Figure 4:** The split into potential and radiative regions (3.20).

There is a nested tadpole integral:

$$\begin{aligned} \int_k \frac{\delta((k-\ell) \cdot v_1)}{(k^2 + \text{sgn}(k^0)i0)^{n_3}} &= \int_{\mathbf{k}} \frac{1}{((\ell \cdot v_1 + i0)^2 - \mathbf{k}^2)^{n_3}} \\ &= \left( \frac{e^{-i\pi}}{4\pi} \right)^{\frac{D-1}{2}} \frac{\Gamma(n_3 - \frac{D-1}{2})}{\Gamma(n_3)} (\ell \cdot v_1 + i0)^{D-1-2n_3}. \end{aligned} \quad (3.26)$$

The retarded massless propagator with power  $n_3$  is turned into a retarded worldline propagator with power  $2n_3 - D + 1$ . An important realization here is that we can obtain  $\text{sgn}(k^0)$  by projecting  $k^\mu$  with any time-like four-vector: so in this case  $\text{sgn}(k^0)i0 = (k \cdot v_1)i0 = (\ell \cdot v_1)i0$  (on support of the  $\delta$ -function constraints). Otherwise one may use the standard tadpole integral, identifying  $(0 - i\ell \cdot v_1) = -i(\ell \cdot v_1 + i0)$  as an imaginary mass.

Integration on the active momentum  $k^\mu$  thus results in additional powers of the retarded worldline propagator. The integral now reads:

$$\begin{aligned} K_{n_1, n_2, n_3, n_4, n_5}^{(+; -; +)} & \\ &= \left( \frac{e^{-i\pi}}{4\pi} \right)^{\frac{D-1}{2}} \frac{\Gamma(n_3 - \frac{D-1}{2})}{\Gamma(n_3)} \int_\ell \frac{\delta(\ell \cdot v_2)}{(\ell \cdot v_1 + i0)^{n_1+2n_3-D+1} (\ell \cdot v_1 - i0)^{n_2} (\ell^2)^{n_4} ((\ell - q)^2)^{n_5}}. \end{aligned} \quad (3.27)$$

This integral is similar to the ones encountered at 2PM [50], the only difference being the presence of both retarded and advanced worldline propagators. It can be integrated directly using Schwinger parametrization, and one finds

$$\begin{aligned} K_{n_1, n_2, n_3, n_4, n_5}^{(+; -; +)} &= (4\pi)^{1-D} \frac{\Gamma(n_3 - \frac{D-1}{2}) \cos(\frac{\pi}{2}(n_1 - n_2 - D + 1))}{\Gamma(n_3) \cos(\frac{\pi}{2}(n_1 + n_2 - D + 1))} \times \\ &(-i)^{n_1 - n_2 + 2n_3 + 2n_4 + 2n_5} \left( \frac{4}{\gamma^2 - 1} \right)^{\frac{n_1 + n_2 + 2n_3 - D + 1}{2}} \Gamma_{n_1 + n_2 + 2n_3 - D + 1, n_4, n_5}(D - 1). \end{aligned} \quad (3.28)$$

The factor  $\Gamma_{n_1, n_2, n_3}(D)$  is given by

$$\Gamma_{n_1, n_2, n_3}(D) := \frac{\Gamma(n_2 + n_3 + \frac{n_1}{2} - \frac{D}{2}) \Gamma(\frac{n_1}{2}) \Gamma(\frac{D}{2} - n_2 - \frac{n_1}{2}) \Gamma(\frac{D}{2} - n_3 - \frac{n_1}{2})}{2\Gamma(n_1) \Gamma(n_2) \Gamma(n_3) \Gamma(D - n_1 - n_2 - n_3)}, \quad (3.29)$$

and arises from the 2PM 1-loop integral — see e.g. ref. [50].

### 3.5 Integral expressions

Here we present expressions for the master integrals of the  $I_{n_1, n_2, \dots, n_7}^{(\sigma_1; \sigma_2; \sigma_3)}$  family. In each case we give results only up to the order in  $\epsilon$  that we find is necessary for producing observables. The b-type master integrals (3.9) are given by<sup>3</sup>

$$\tilde{\mathcal{I}}_1 = \tilde{\mathcal{I}}'_1 = \tilde{\mathcal{I}}''_1 = \mathcal{O}(\epsilon^2), \quad (3.30a)$$

$$\tilde{\mathcal{I}}_2 = \tilde{\mathcal{I}}'_2 = \tilde{\mathcal{I}}''_2 = \frac{\epsilon}{2} \log(x) + \mathcal{O}(\epsilon^2), \quad (3.30b)$$

$$\tilde{\mathcal{I}}_3 = \tilde{\mathcal{I}}'_3 = \tilde{\mathcal{I}}''_3 = -\frac{1}{2} + \mathcal{O}(\epsilon), \quad (3.30c)$$

$$\tilde{\mathcal{I}}_4 = \tilde{\mathcal{I}}'_4 = \tilde{\mathcal{I}}''_4 = -\frac{1}{2} + \mathcal{O}(\epsilon), \quad (3.30d)$$

$$\tilde{\mathcal{I}}_5 = \tilde{\mathcal{I}}'_5 = \tilde{\mathcal{I}}''_5 = \frac{1}{2} + \mathcal{O}(\epsilon), \quad (3.30e)$$

$$\tilde{\mathcal{I}}_6 = \tilde{\mathcal{I}}'_6 = \tilde{\mathcal{I}}''_6 = -\epsilon \log(x) + \mathcal{O}(\epsilon^2), \quad (3.30f)$$

$$\tilde{\mathcal{I}}_7 = \tilde{\mathcal{I}}'_7 = \tilde{\mathcal{I}}''_7 = \mathcal{O}(\epsilon^2), \quad (3.30g)$$

$$\tilde{\mathcal{I}}_8 = -\frac{1}{2} + \frac{\epsilon}{2} \log(x) + \mathcal{O}(\epsilon^2), \quad (3.30h)$$

$$\tilde{\mathcal{I}}'_8 = -\frac{1}{2} + \frac{\epsilon}{2} \log(x) + \mathcal{O}(\epsilon^2), \quad (3.30i)$$

$$\tilde{\mathcal{I}}''_8 = 1 + \frac{\epsilon}{2} \log(x) + \mathcal{O}(\epsilon^2), \quad (3.30j)$$

with the normalization  $\tilde{\mathcal{I}}_i := (4\pi)^{2-2\epsilon} e^{2\gamma_E \epsilon} \mathcal{I}_i$ . As expected, all of these are real in the physical region  $0 < x < 1$ : the first seven are given by the real part of the corresponding integrals with Feynman  $i0$  prescription [97], which carry both real and imaginary parts when evaluated in the physical region. The v-type integrals are

$$\tilde{\mathcal{I}}_9 = \tilde{\mathcal{I}}''_9 = \mathcal{O}(\epsilon^0), \quad (3.31a)$$

$$\tilde{\mathcal{I}}_{10} = \tilde{\mathcal{I}}''_{10} = +\frac{i\pi}{2} - i\pi \log(2x)\epsilon + \mathcal{O}(\epsilon^2), \quad (3.31b)$$

$$\tilde{\mathcal{I}}_{11} = \tilde{\mathcal{I}}'_{11} = \tilde{\mathcal{I}}''_{11} = -\frac{i\pi}{6} - \frac{i\pi}{3}(\log(8x) - \log(1-x^2))\epsilon + \mathcal{O}(\epsilon^2), \quad (3.31c)$$

$$\tilde{\mathcal{I}}_{12} = \tilde{\mathcal{I}}'_{12} = \tilde{\mathcal{I}}''_{12} = +\frac{i\pi}{4} - \frac{i\pi}{2}(\log(2x) + \log(1-x) - 3\log(1+x))\epsilon + \mathcal{O}(\epsilon^2), \quad (3.31d)$$

$$\tilde{\mathcal{I}}_{13} = \tilde{\mathcal{I}}'_{13} = \tilde{\mathcal{I}}''_{13} = -\frac{i\pi}{2}(\log(4x) - 2\log(1+x))\epsilon + \mathcal{O}(\epsilon^2), \quad (3.31e)$$

$$\tilde{\mathcal{I}}'_9 = \tilde{\mathcal{I}}''_{14} = \mathcal{O}(\epsilon^0), \quad (3.31f)$$

$$\tilde{\mathcal{I}}'_{10} = \tilde{\mathcal{I}}''_{15} = -\frac{i\pi}{2} - i\pi \log\left(\frac{x}{2}\right)\epsilon + \mathcal{O}(\epsilon^2), \quad (3.31g)$$

and as expected are purely imaginary. We see that  $\mathcal{I}_i = \mathcal{I}'_i$  for  $11 \leq i \leq 13$ , which is due to all three of these integrals vanishing in the potential region: this gives rise to an additional “hidden” symmetry. When assembling physical observables,  $\log(1-x)$  generically cancels between the integrals  $\mathcal{I}_{11}$  and  $\mathcal{I}_{12}$ . This gives rise to the two commonly occurring combinations:

$$\operatorname{arccosh} \gamma = -\log(x), \quad (3.32a)$$

$$\log\left(\frac{\gamma+1}{2}\right) = 2\log(1+x) - \log(4x), \quad (3.32b)$$

---

<sup>3</sup>We thank Gregor Kälin for checking the  $\mathcal{I}_5$  integral.

which we will use to present our results in section 4 in a compact manner.

## 4 Radiation-reacted tidal effects

With the technology for performing retarded integrals at 3PM order now established, let us use it to derive gravitational observables from a scattering event. We focus on the inclusion of tidal effects in the point-particle action:

$$S_{\text{pp}}^{(i)} + S_{\text{tidal}}^{(i)} = m_i \int d\tau \left[ -\frac{1}{2} g_{\mu\nu} \dot{x}_i^\mu \dot{x}_i^\nu + c_{E^2}^{(i)} E_{\mu\nu}^{(i)} E^{(i)\mu\nu} + c_{B^2}^{(i)} B_{\mu\nu}^{(i)} B^{(i)\mu\nu} \right], \quad (4.1)$$

where  $c_{E^2}^{(i)}$  and  $c_{B^2}^{(i)}$  are the quadrupole Love numbers and  $E_{\mu\nu}^{(i)} := R_{\mu\alpha\nu\beta} \dot{x}_i^\alpha \dot{x}_i^\beta$ ,  $B_{\mu\nu}^{(i)} := R_{\mu\alpha\nu\beta}^* \dot{x}_i^\alpha \dot{x}_i^\beta$  are the electromagnetic curvature tensors with  $R_{\mu\alpha\nu\beta}^* := \frac{1}{2} \epsilon_{\nu\beta\rho\sigma} R_{\mu\alpha}{}^{\rho\sigma}$ . As explained in refs. [47, 50], we read off Feynman rules by expressing the constituent fields in Fourier space:  $h_{\mu\nu}(x) = \int_k e^{-ik \cdot x} h_{\mu\nu}(k)$  and  $z_i^\mu(\tau) = \int_\omega e^{-i\omega\tau} z_i^\mu(\omega)$ . Interaction vertices stemming from the point-particle action involve only a single graviton:

$$z^{\rho_1}(\omega_1) = i^{n-1} m \kappa e^{ik \cdot b} \bar{\delta} \left( k \cdot v + \sum_{i=1}^n \omega_i \right) \times \quad (4.2)$$

$$h_{\mu\nu}(k) \left( \frac{1}{2} \left( \prod_{i=1}^n k_{\rho_i} \right) v^\mu v^\nu + \sum_{i=1}^n \omega_i \left( \prod_{j \neq i}^n k_{\rho_j} \right) v^{(\mu} \delta_{\rho_i}^{\nu)} + \sum_{i < j}^n \omega_i \omega_j \left( \prod_{l \neq i, j}^n k_{\rho_l} \right) \delta_{\rho_i}^{(\mu} \delta_{\rho_j}^{\nu)} \right),$$

while those arising from the tidal corrections involve a minimum of two gravitons:

$$z^{\rho_1}(\omega_1) = 2i^{n+1} m \kappa^2 e^{iq \cdot b} \bar{\delta} \left( q \cdot v + \sum_{i=1}^n \omega_i \right) \times \quad (4.3a)$$

$$h_{\mu_1 \nu_1}(k_1) h_{\mu_2 \nu_2}(k_2) \left[ c_{E^2}^{(i)} R^{(1)}{}_{\epsilon\alpha\delta\beta, \mu_1 \nu_1} R^{(1)}{}_{\gamma \xi}{}^{\alpha \beta}{}_{, \mu_2 \nu_2} + c_{B^2}^{(i)} R^{*(1)}{}_{\epsilon\alpha\delta\beta, \mu_1 \nu_1} R^{*(1)}{}_{\gamma \xi}{}^{\alpha \beta}{}_{, \mu_2 \nu_2} \right] T^{\epsilon\delta\gamma\xi}{}_{\rho_1 \dots \rho_n},$$

$$z^{\rho_1}(\omega_1) = i^{n+1} m \kappa^3 e^{iq \cdot b} \bar{\delta} \left( q \cdot v + \sum_{i=1}^n \omega_i \right) \times \quad (4.3b)$$

$$h_{\mu_1 \nu_1}(k_1) h_{\mu_2 \nu_2}(k_2) h_{\mu_3 \nu_3}(k_3) \sum_{\sigma \in S_3} \left[ c_{E^2}^{(i)} \left( R^{(2)}{}_{\epsilon\alpha\delta\beta, \mu_{\sigma_1} \nu_{\sigma_1} \mu_{\sigma_2} \nu_{\sigma_2}} R^{(1)}{}_{\gamma \xi}{}^{\alpha \beta}{}_{, \mu_{\sigma_3} \nu_{\sigma_3}} + R^{(1)}{}_{\epsilon\alpha\delta\beta, \mu_{\sigma_1} \nu_{\sigma_1}} R^{(2)}{}_{\gamma \xi}{}^{\alpha \beta}{}_{, \mu_{\sigma_2} \nu_{\sigma_2} \mu_{\sigma_3} \nu_{\sigma_3}} \right) + c_{B^2}^{(i)} \left( R^{*(2)}{}_{\epsilon\alpha\delta\beta, \mu_{\sigma_1} \nu_{\sigma_1} \mu_{\sigma_2} \nu_{\sigma_2}} R^{*(1)}{}_{\gamma \xi}{}^{\alpha \beta}{}_{, \mu_{\sigma_3} \nu_{\sigma_3}} + R^{*(1)}{}_{\epsilon\alpha\delta\beta, \mu_{\sigma_1} \nu_{\sigma_1}} R^{*(2)}{}_{\gamma \xi}{}^{\alpha \beta}{}_{, \mu_{\sigma_2} \nu_{\sigma_2} \mu_{\sigma_3} \nu_{\sigma_3}} \right) \right] T^{\epsilon\delta\gamma\xi}{}_{\rho_1 \dots \rho_n}.$$



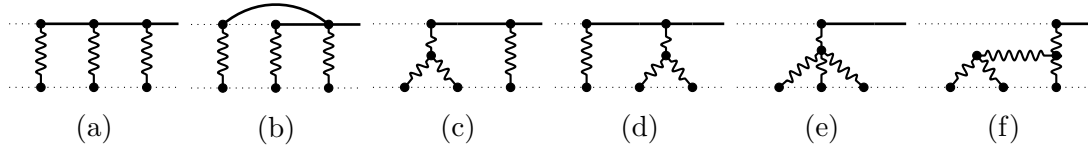


**Figure 5:** The six diagrams contributing to the  $m_1 m_2^3$  component of  $\Delta p_1^{(3)\mu}$  in the absence of tidal corrections. The upper worldline is one continuous fluctuation and hence we have test-body motion.

Both expressions include

$$\begin{aligned}
T^{\epsilon\sigma\gamma\xi}_{\rho_1\dots\rho_n} &= \left( \prod_{i=1}^n q_{\rho_i} \right) v^\epsilon v^\sigma v^\gamma v^\xi + 4 \sum_{i=1}^n \omega_i \left( \prod_{j \neq i}^n q_{\rho_j} \right) v^{(\epsilon} v^\sigma v^\gamma \delta_{\rho_i}^{\xi)} \\
&+ 24 \sum_{i < j}^n \omega_i \omega_j \left( \prod_{k \neq i, j}^n q_{\rho_k} \right) v^{(\epsilon} v^\sigma \delta_{\rho_i}^\gamma \delta_{\rho_j}^{\xi)} + 24 \sum_{i < j < k}^n \omega_i \omega_j \omega_k \left( \prod_{l \neq i, j, k}^n q_{\rho_l} \right) v^{(\epsilon} \delta_{\rho_i}^\sigma \delta_{\rho_j}^\gamma \delta_{\rho_k}^{\xi)} \\
&+ 24 \sum_{i < j < k < l}^n \omega_i \omega_j \omega_k \omega_l \left( \prod_{m \neq i, j, k, l}^n q_{\rho_m} \right) \delta_{\rho_i}^{(\epsilon} \delta_{\rho_j}^\sigma \delta_{\rho_k}^\gamma \delta_{\rho_l}^{\xi)}, \tag{4.4}
\end{aligned}$$

where  $q^\mu = \sum_i k_i^\mu$  is the total momentum of all emitted gravitons and

$$R^{(n)}_{\alpha\beta\rho\sigma, \mu_1\nu_1\dots\mu_n\nu_n} := \frac{\delta^n R^{(n)}_{\alpha\beta\rho\sigma}}{\delta h^{\mu_1\nu_1} \dots \delta h^{\mu_n\nu_n}}. \tag{4.5}$$

$R^{(n)}_{\alpha\beta\rho\sigma}$  is given by the  $n$ 'th order of  $\kappa = \sqrt{32\pi G}$  in a PM expansion of the curvature tensor where we replace the graviton field by its Fourier transform  $h_{\mu\nu}(x) \rightarrow h_{\mu\nu}(-k)$ , and similarly for the dual of the curvature tensor. The complete set of Feynman rules also includes bulk interactions arising from the  $D$ -dimensional Einstein-Hilbert action and gauge-fixing term:

$$S_{\text{EH}} = -\frac{2}{\kappa^2} \int d^D x \sqrt{-g} R, \quad S_{\text{gf}} = \int d^D x \left( \partial_\nu h^{\mu\nu} - \frac{1}{2} \partial^\mu h^\nu{}_\nu \right)^2, \tag{4.6}$$

where the gauge-fixing constraint is  $\partial_\nu h^{\mu\nu} = \frac{1}{2} \partial^\mu h^\nu{}_\nu$ . Expressions for the retarded graviton and worldline propagators were provided in eqs. (2.24) and (2.25).

#### 4.1 Impulse

Our main goal is to calculate the impulse (deflection) on the first body, including radiation-reaction effects. This is recovered from the WQFT using:

$$\Delta p_1^\mu = -m_1 \omega^2 \langle z_1^\mu(\omega) \rangle|_{\omega=0}, \tag{4.7}$$

where the expectation value was discussed in eq. (2.29) and  $\Delta p_i^\mu = \sum_n G^n \Delta p_i^{(n)\mu}$  in the PM expansion. As the results for  $\Delta p_i^{(1)\mu}$  and  $\Delta p_i^{(2)\mu}$  are well-established — tidal

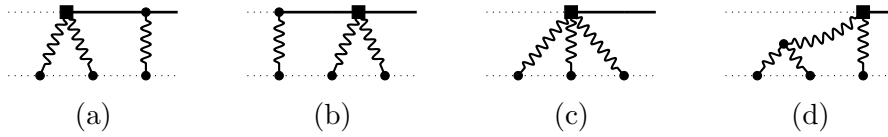


**Figure 6:** The four types of diagrams contributing to the test-body  $m_1 m_2^3$  components of  $\Delta p_1^{(3)\mu}$  linear in tidal coefficients.

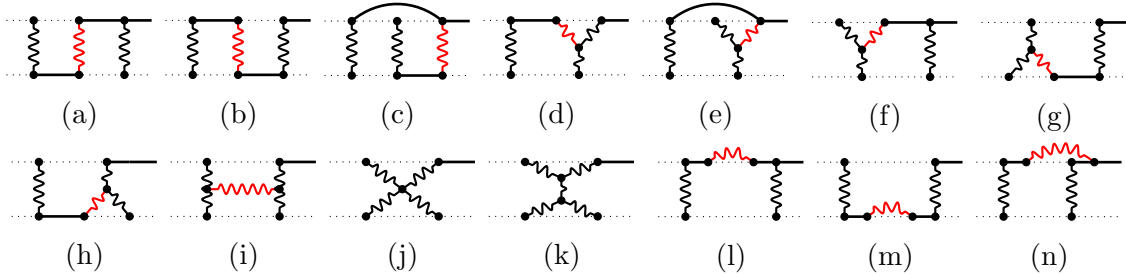


**Figure 7:** The 14 types of diagrams contributing to the  $m_1^2 m_2^2$  components of the 3PM gravitational impulse  $\Delta p_1^{(3)\mu}$  without tidal corrections. All diagrams except the last, (n), are associated with the comparable-mass family  $I_{n_1, n_2, \dots, n_7}^{(\sigma_1; \sigma_2; \sigma_3)}$  (3.1); diagrams (l)–(n) are associated with  $K_{n_1, n_2, \dots, n_5}^{(\sigma_1; \sigma_2; \sigma_3)}$  family (3.25).

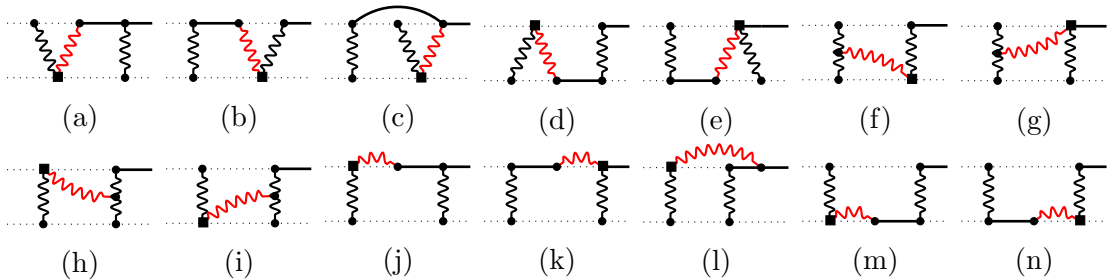


**Figure 8:** The 14 types of diagrams contributing to the  $m_1^2 m_2^2$  comparable-mass components of  $\Delta p_1^{(3)\mu}$  linear in tidal coefficients.

effects beginning at 2PM order [38, 110–112] — we focus here on the 3PM component  $\Delta p_i^{(3)\mu}$ . This will allow us to use the retarded integrals derived in section 3. Results for  $\Delta p_i^{(1)\mu}$  and  $\Delta p_i^{(2)\mu}$  are included in the ancillary file attached to the arXiv submission of this paper.

We proceed by drawing all diagrams with a single (cut) outgoing  $z_1^\mu$  line. There are four categories of diagrams, displayed in Figs. 5–8. All retarded propagators, both in the bulk and on the worldlines, point towards the outgoing line: from cause to effect. In particular: Figs. 5 and 6 contain the contributions to  $\Delta p_i^{(3)\mu}$  in the test-body limit  $m_1 \ll m_2$ , with and without the tidal corrections respectively. These involve the integral family  $J_{n_1, n_2, \dots, n_7}^{(\sigma_1; \sigma_2)}$ , consisting only of potential modes. Figs. 7 and 8 contain the comparable-mass diagrams. These latter contributions are modified

by the inclusion of radiative effects, and involve the integral families  $I_{n_1, n_2, \dots, n_7}^{(\sigma_1; \sigma_2; \sigma_3)}$  and  $K_{n_1, n_2, \dots, n_5}^{(\sigma_1; \sigma_2; \sigma_3)}$  discussed in section 3. There is also a third category of diagrams (not drawn) relevant in the other test-body limit  $m_1 \gg m_2$ ; however, as these are related by symmetry to those in Figs. 5 and 6 we do not need to calculate them explicitly.

All integrands can be expressed as a Fourier transform over integrals of the kind discussed in section 3:

$$\int_q e^{iq \cdot b} \bar{\delta}(q \cdot v_1) \bar{\delta}(q \cdot v_2) |q|^n \{ I_{n_1, \dots, n_7}^{(\sigma_1; \sigma_2; \sigma_3)}, J_{n_1, \dots, n_7}^{(\sigma_1; \sigma_2)}, K_{n_1, \dots, n_5}^{(\sigma_1; \sigma_2; \sigma_3)} \}, \quad (4.8)$$

where  $q^\mu$  is the total momentum exchanged via gravitons between the two worldlines. To bring the diagrams into this form, we need to resolve four-dimensional delta functions in the bulk and integrate over the energies  $\omega_i$  of worldline propagators. As explained in ref. [51], any leftover components of  $\ell_i^\mu$  may be conveniently resolved on a basis of  $w_i^\mu$  and  $q^\mu$ , where  $w_i^\mu$  are the dual velocities satisfying  $v_i \cdot w_j = \delta_{ij}$ :

$$w_1^\mu = \frac{\gamma v_2^\mu - v_1^\mu}{\gamma^2 - 1}, \quad w_2^\mu = \frac{\gamma v_1^\mu - v_2^\mu}{\gamma^2 - 1}. \quad (4.9)$$

After reducing to the master integrals given in section 3.5, our last step is to perform the  $q$ -Fourier transform.

Our final result for  $\Delta p_1^\mu$  up to 3PM order is given in the ancillary file. It takes the generic form [32]:

$$\Delta p_1^\mu = p_\infty \sin \theta \frac{b^\mu}{|b|} + (\cos \theta - 1) \frac{m_1 m_2}{E^2} [(\gamma m_1 + m_2) v_1^\mu - (\gamma m_2 + m_1) v_2^\mu] - v_2 \cdot P_{\text{rad}} w_2^\mu, \quad (4.10)$$

where the center-of-mass momentum is  $p_\infty = \mu \sqrt{\gamma^2 - 1} / \Gamma$ ,  $\mu = M\nu = m_1 m_2 / M$ ,  $M = m_1 + m_2$  and  $\Gamma = E / M = \sqrt{1 + 2\nu(\gamma - 1)}$ . All terms proportional to the impact parameter  $b^\mu$ , both conservative and radiative, arise from the real integrals (3.30); terms proportional to  $v_i^\mu$ , including  $P_{\text{rad}}^\mu$ , come from the imaginary integrals (3.31). Here  $\theta$  is the scattering angle in the center-of-mass frame, and  $P_{\text{rad}}^\mu$  is the radiated four-momentum:

$$\sin \left( \frac{\theta}{2} \right) = \frac{\sqrt{-\Delta p_1^2}}{2p_\infty}, \quad P_{\text{rad}}^\mu = -\Delta p_1^\mu - \Delta p_2^\mu. \quad (4.11)$$

The entire dynamics is therefore encoded by  $\theta$  and  $P_{\text{rad}}^\mu$ , which we present below.

## 4.2 Scattering angle

In the absence of tidal effects, the complete scattering angle  $\theta$  up to  $\mathcal{O}(G^3)$  is

$$\begin{aligned} \frac{\theta_{\text{cons}}}{\Gamma} &= \frac{GM}{|b|} \frac{2(2\gamma^2 - 1)}{\gamma^2 - 1} + \left(\frac{GM}{|b|}\right)^2 \frac{3\pi(5\gamma^2 - 1)}{4(\gamma^2 - 1)} \\ &+ \left(\frac{GM}{|b|}\right)^3 \left( 2 \frac{64\gamma^6 - 120\gamma^4 + 60\gamma^2 - 5}{3(\gamma^2 - 1)^3} \Gamma^2 \right. \\ &\quad \left. - \frac{8\nu\gamma(14\gamma^2 + 25)}{3(\gamma^2 - 1)} - 8\nu \frac{(4\gamma^4 - 12\gamma^2 - 3) \operatorname{arccosh}\gamma}{(\gamma^2 - 1) \sqrt{\gamma^2 - 1}} \right) + \mathcal{O}(G^4), \end{aligned} \quad (4.12a)$$

$$\frac{\theta_{\text{rad}}}{\Gamma} = \left(\frac{GM}{|b|}\right)^3 \frac{4\nu(2\gamma^2 - 1)^2}{(\gamma^2 - 1)^{3/2}} \left( -\frac{8}{3} + \frac{1}{v^2} + \frac{(3v^2 - 1)}{v^3} \operatorname{arccosh}\gamma \right) + \mathcal{O}(G^4), \quad (4.12b)$$

where  $\theta = \theta_{\text{cons}} + \theta_{\text{rad}}$  has a finite high-energy  $\gamma \rightarrow \infty$  limit:

$$\theta \xrightarrow{\gamma \rightarrow \infty} 4 \frac{GE}{|b|} + \frac{32}{3} \left(\frac{GE}{|b|}\right)^3. \quad (4.13)$$

This is the well-known result of Amati, Ciafaloni and Veneziano [113], the radiative correction  $\theta_{\text{rad}}$  being required in order to cancel a logarithmic divergence that otherwise appears in this limit [78]. With the inclusion of tidal effects, only the conservative part of the angle is modified up to 3PM order, i.e.  $\theta_{\text{tidal}} = \theta_{\text{tidal,cons}} + \mathcal{O}(G^4)$ :

$$\begin{aligned} \frac{\theta_{\text{tidal}}}{\Gamma} &= \frac{45\pi G^2 M^2}{128|b|^6(\gamma^2 - 1)} \left[ (11 - 30\gamma^2 + 35\gamma^4) (c_{E^2}^+ - \delta c_{E^2}^-) \right. \\ &\quad \left. + (-5 - 30\gamma^2 + 35\gamma^4) (c_{B^2}^+ - \delta c_{B^2}^-) \right] \\ &+ \frac{48G^3 M^3}{|b|^7(\gamma^2 - 1)^2} \left[ \frac{1}{35} (-5 + 72\gamma^2 - 192\gamma^4 + 160\gamma^6) ((1 + \delta^2)c_{E^2}^+ - 2\delta c_{E^2}^-) \right. \\ &\quad + \frac{1}{35} (2 + 30\gamma^2 - 192\gamma^4 + 160\gamma^6) ((1 + \delta^2)c_{B^2}^+ - 2\delta c_{B^2}^-) \\ &\quad + \frac{2\nu\gamma}{5(\gamma^2 - 1)} (4047 + 9426\gamma^2 + 804\gamma^4 - 104\gamma^6 + 32\gamma^8) c_{E^2}^+ \\ &\quad + \frac{4\nu\gamma}{5(\gamma^2 - 1)} (2006 + 4733\gamma^2 + 392\gamma^4 - 52\gamma^6 + 16\gamma^8) c_{B^2}^+ \\ &\quad \left. - \frac{6\nu}{\gamma^2 - 1} \frac{\operatorname{arccosh}\gamma}{\sqrt{\gamma^2 - 1}} \left[ (33 + 474\gamma^2 + 440\gamma^4) c_{E^2}^+ \right. \right. \\ &\quad \left. \left. + (32 + 474\gamma^2 + 440\gamma^4) c_{B^2}^+ \right] \right] + \mathcal{O}(G^4), \end{aligned}$$

with  $\delta = (m_2 - m_1)/M$  and  $c_{E^2/B^2}^\pm = c_{E^2/B^2}^{(2)} \pm c_{E^2/B^2}^{(1)}$  — see also refs. [38, 112]. It has a finite high-energy limit:

$$\theta_{\text{tidal}} \xrightarrow{\gamma \rightarrow \infty} \left(\frac{GE}{|b|}\right)^7 \frac{384(\kappa_{E^2} + \kappa_{B^2})}{5\nu^2}, \quad \kappa_{E^2/B^2} = \frac{c_{E^2/B^2}^+}{G^4 M^4}, \quad (4.14)$$

where the dimensionless parameters  $\kappa_{E^2/B^2}$  account for the mass dependence of the Love numbers  $c_{E^2/B^2}^{(a)}$ .

The absence of a radiative part of the tidal correction to the scattering angle at 3PM order is explained using the linear response relation [78, 114, 115]:

$$\theta_{\text{rad}} = -\frac{1}{2} \frac{\partial \theta_{\text{cons}}}{\partial E} E_{\text{rad}} - \frac{1}{2} \frac{\partial \theta_{\text{cons}}}{\partial J} J_{\text{rad}}. \quad (4.15)$$

This predicts the radiative part of the scattering angle  $\theta_{\text{rad}}$  given knowledge of the radiated energy  $E_{\text{rad}}$  and angular momentum  $J_{\text{rad}}$ . As  $E_{\text{rad}} = P_{\text{rad}}^0$  (in the center-of-mass frame) begins at 3PM order, to deduce the 3PM contribution to  $\theta_{\text{rad}}$  we need only  $J_{\text{rad}}$  at 2PM order. As we shall see in section 4.4, the absence of a *wave memory* in the tidal correction to the 2PM waveform guarantees that  $J_{\text{tidal,rad}} = \mathcal{O}(G^3)$ , hence  $\theta_{\text{tidal,rad}} = \mathcal{O}(G^4)$ .

### 4.3 Radiated momentum

The radiated four-momentum without finite-size effects up to  $\mathcal{O}(G^3)$  is (see also refs. [42, 80, 96]):

$$P_{\text{rad}}^\mu = \frac{G^3 m_1^2 m_2^2 \pi}{|b|^3} \frac{v_1^\mu + v_2^\mu}{\gamma + 1} \mathcal{E}(\gamma) + \mathcal{O}(G^4), \quad (4.16)$$

with the scalar function  $\mathcal{E}(\gamma)$  giving the radiated energy in the center-of-mass (com) frame  $E_{\text{rad}} = P_{\text{rad}} \cdot v_{\text{com}} = P_{\text{rad}} \cdot (m_1 v_1^\mu + m_2 v_2^\mu)/E$ :

$$E_{\text{rad}} = \frac{G^3 \pi M^4 \nu^2}{|b|^3 \Gamma} \mathcal{E}(\gamma), \quad \mathcal{E}(\gamma) = e_1 + e_2 \log\left(\frac{\gamma + 1}{2}\right) + e_3 \frac{\text{arccosh} \gamma}{\sqrt{\gamma^2 - 1}}. \quad (4.17)$$

The coefficients are

$$e_1 = \frac{210\gamma^6 - 552\gamma^5 + 339\gamma^4 - 912\gamma^3 + 3148\gamma^2 - 3336\gamma + 1151}{48(\gamma^2 - 1)^{3/2}}, \quad (4.18a)$$

$$e_2 = -\frac{35\gamma^4 + 60\gamma^3 - 150\gamma^2 + 76\gamma - 5}{8\sqrt{\gamma^2 - 1}}, \quad (4.18b)$$

$$e_3 = \frac{\gamma(2\gamma^2 - 3)(35\gamma^4 - 30\gamma^2 + 11)}{16(\gamma^2 - 1)^{3/2}}. \quad (4.18c)$$

Incorporating leading-order tidal effects the correction to the radiated four-momentum  $P_{\text{rad,tidal}}^\mu$  at this order is given by

$$P_{\text{rad,tidal}}^\mu = \frac{G^3 \pi m_1^2 m_2^2}{|b|^7} \left[ \left( c_{E^2}^{(1)} \mathcal{A}_{E^2} + c_{E^2}^{(2)} \mathcal{B}_{E^2} + c_{B^2}^{(1)} \mathcal{A}_{B^2} + c_{B^2}^{(2)} \mathcal{B}_{B^2} \right) \frac{\gamma v_2^\mu - v_1^\mu}{\sqrt{\gamma^2 - 1}} + (1 \leftrightarrow 2) \right], \quad (4.19)$$

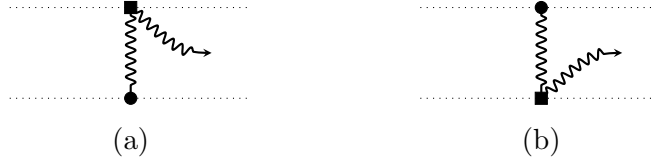


**Figure 9:** The two diagrams contributing to tidal effects at  $\mathcal{O}(G^2)$  to the waveform

and the scalar factors  $\mathcal{A}_x$  depend only on  $\gamma$ :

$$\mathcal{A}_x = a_{1,x} + a_{2,x} \log\left(\frac{\gamma+1}{2}\right) + a_{3,x} \frac{\operatorname{arccosh}\gamma}{\sqrt{\gamma^2-1}}, \quad (4.20a)$$

$$a_{1,E^2} = \frac{15}{128(\gamma-1)(\gamma+1)^4} (937\gamma^9 + 1551\gamma^8 - 2463\gamma^7 - 5645\gamma^6 + 20415\gamma^5 + 65965\gamma^4 - 349541\gamma^3 + 535057\gamma^2 - 360356\gamma + 92160), \quad (4.20b)$$

$$a_{1,B^2} = \frac{15}{256(\gamma+1)^4} (1559\gamma^8 + 3716\gamma^7 - 1630\gamma^6 - 11660\gamma^5 + 28288\gamma^4 + 155292\gamma^3 - 543442\gamma^2 + 535212\gamma - 180775), \quad (4.20c)$$

$$a_{2,E^2} = \frac{225}{32} (21\gamma^4 - 14\gamma^2 + 9), \quad (4.20d)$$

$$a_{2,B^2} = \frac{1575}{32} (3\gamma^4 - 2\gamma^2 - 1), \quad (4.20e)$$

$$a_{3,x} = -\frac{\gamma(2\gamma^2-3)}{4(\gamma^2-1)} a_{2,x}. \quad (4.20f)$$

Finally,  $\mathcal{B}_x$  are rational functions of  $\gamma$ :

$$\mathcal{B}_{E^2} = \frac{45(\gamma-1)}{64(\gamma+1)^4} (42\gamma^8 + 210\gamma^7 + 315\gamma^6 - 105\gamma^5 - 944\gamma^4 - 1528\gamma^3 + 22011\gamma^2 - 33201\gamma + 16272), \quad (4.21a)$$

$$\mathcal{B}_{B^2} = -\frac{45(\gamma-1)^2(105\gamma^5 + 630\gamma^4 + 1840\gamma^3 + 3690\gamma^2 - 17769\gamma + 15984)}{64(\gamma+1)^4}. \quad (4.21b)$$

The tidal correction to the radiated energy is given by

$$E_{\text{rad,tidal}} = \frac{G^3 \pi M^3 \nu^2 \sqrt{\gamma^2-1}}{|b|^7 \Gamma} \left[ \mathcal{A}_{E^2} (m_1 c_{E^2}^{(1)} + m_2 c_{E^2}^{(2)}) + \mathcal{B}_{E^2} (m_1 c_{E^2}^{(2)} + m_2 c_{E^2}^{(1)}) + \mathcal{A}_{B^2} (m_1 c_{B^2}^{(1)} + m_2 c_{B^2}^{(2)}) + \mathcal{B}_{B^2} (m_1 c_{B^2}^{(2)} + m_2 c_{B^2}^{(1)}) \right]. \quad (4.22)$$

These results all agree with ref. [43].

#### 4.4 Waveform

As a final application of the new WQFT Feynman rules (4.3) we compute the leading-order  $G^2$  gravitational waveform produced by a scattering of two compact objects,

corrected by tidal effects. This result was also recently obtained in ref. [43] — besides its inherent usefulness, it provides us with a means to check the radiated linear momentum  $P_{\text{rad}}^\mu$  (4.16) and confirm that the correction to the radiated angular momentum  $J_{\text{rad}}$  from tidal effects vanishes at leading order  $\mathcal{O}(G^2)$ . Following refs. [48, 49] the gauge-invariant frequency-domain waveform  $4G \epsilon^{\mu\nu} S_{\mu\nu}(k^\mu = \Omega \rho^\mu)$  is extracted from the WQFT via

$$S_{\mu\nu}(k) = \frac{2}{\kappa} k^2 \langle h_{\mu\nu}(k) \rangle, \quad (4.23)$$

where  $\Omega$  is the gravitational wave frequency and  $\rho^\mu = (1, \hat{\mathbf{x}})$ ,  $\hat{\mathbf{x}} := \mathbf{x}/r$  being a unit vector pointing towards the observer. We work in the *wave zone*, where  $r = |\mathbf{x}|$  is much larger than all other length scales in the problem.

We find it advantageous to study the time-domain waveform  $f(u, \hat{\mathbf{x}})$ , which is given by a Fourier transform:

$$\kappa \epsilon^{\mu\nu} h_{\mu\nu} = \frac{f(u, \hat{\mathbf{x}})}{r} = \frac{4G}{r} \int_{\Omega} e^{-i\Omega u} \epsilon^{\mu\nu} S_{\mu\nu}(k) \Big|_{k^\mu = \Omega \rho^\mu}, \quad (4.24)$$

and  $u = t - r$  is the retarded time. The polarization tensor factorizes as  $\epsilon^{\mu\nu} = \frac{1}{2} \epsilon^\mu \epsilon^\nu$ , where  $\epsilon \cdot \epsilon = \epsilon \cdot \rho = 0$ ; in a PM decomposition  $f = \sum_n G^n f^{(n)}$  we seek the 2PM component  $f^{(2)}$ . As the time-domain waveform in the absence of tidal effects has already been computed in refs. [41, 48, 49], we focus here only on the tidal corrections. The two contributing diagrams are drawn in Fig. 9.

The integrals required are simpler than those used in refs. [48, 49]: we require only derivatives with respect to  $\tilde{b}^\mu$  of

$$\int_q \delta(q \cdot v_1) \frac{e^{-iq \cdot \tilde{b}}}{q^2} = -\frac{1}{4\pi |\tilde{\mathbf{b}}|_1}, \quad (4.25)$$

where  $\tilde{b}^\mu$  is the shifted impact parameter:

$$\tilde{b}^\mu = \tilde{b}_2^\mu - \tilde{b}_1^\mu, \quad \tilde{b}_i^\mu = b_i^\mu + u_i v_i^\mu, \quad u_i = \frac{\rho \cdot (x - b_i)}{\rho \cdot v_i}, \quad (4.26)$$

and  $u_i$  is the retarded time in the rest frame of the  $i$ 'th body. We have also introduced

$$|\tilde{\mathbf{b}}|_{1,2} := \sqrt{-\tilde{b}_\mu P_{1,2}^{\mu\nu} \tilde{b}_\nu} = \sqrt{|b|^2 + (\gamma^2 - 1) u_{2,1}^2}, \quad (4.27)$$

which are the lengths of the shifted impact parameter  $\tilde{b}^\mu$  in the two rest frames, and  $P_i^{\mu\nu} = \eta^{\mu\nu} - v_i^\mu v_i^\nu$ . The tidal correction to the waveform  $f = \sum_n G^n f^{(n)}$  is given by:

$$f_{\text{tidal}}^{(2)} = m_1 m_2 \frac{c_{E^2}^{(1)} W_{1,E^2} + c_{B^2}^{(1)} W_{1,B^2}}{(|\tilde{\mathbf{b}}|_2)^9} + (1 \leftrightarrow 2), \quad (4.28)$$

where the coefficients are given by

$$\begin{aligned}
W_{1,E^2} = & -12(\gamma^2 - 1)|b|^2(-10u_1(b \cdot \epsilon v_1 \cdot \rho + u_2 v_1 \cdot \epsilon v_2 \cdot \rho) \\
& \times [-3\gamma v_1 \cdot \rho v_2 \cdot \epsilon (2\gamma^2 - 1)v_1 \cdot \rho v_1 \cdot \epsilon + 3\gamma v_1 \cdot \epsilon v_2 \cdot \rho] \\
& + 5(2\gamma^2 - 1)[b \cdot \epsilon v_1 \cdot \rho + u_2 v_1 \cdot \epsilon v_2 \cdot \rho]^2 \\
& - [u_1^2(3(10\gamma^2 - 17)(v_1 \cdot \rho)^2(v_2 \cdot \epsilon)^2 \\
& + (v_1 \cdot \epsilon)^2((5 - 10\gamma^2)(v_1 \cdot \rho)^2 - 30\gamma v_1 \cdot \rho v_2 \cdot \rho + 3(10\gamma^2 - 17)(v_2 \cdot \rho)^2) \\
& + 6v_1 \cdot \rho v_1 \cdot \epsilon v_2 \cdot \epsilon(5\gamma v_1 \cdot \rho + (17 - 10\gamma^2)v_2 \cdot \rho)]) \\
& + 24(\gamma^2 - 1)^2 u_1^2(-10u_1[b \cdot \epsilon v_1 \cdot \rho + u_2 v_1 \cdot \epsilon v_2 \cdot \rho] \\
& \times [-2\gamma v_1 \cdot \rho v_2 \cdot \epsilon + (6\gamma^2 - 3)v_1 \cdot \rho v_1 \cdot \epsilon + 2\gamma v_1 \cdot \epsilon v_2 \cdot \rho] \\
& + 15(2\gamma^2 - 1)[b \cdot \epsilon v_1 \cdot \rho + u_2 v_1 \cdot \epsilon v_2 \cdot \rho]^2 \\
& + u_1^2[6(v_1 \cdot \rho)^2(v_2 \cdot \epsilon)^2 + (v_1 \cdot \epsilon)^2(15(2\gamma^2 - 1)(v_1 \cdot \rho)^2 \\
& + 20\gamma v_1 \cdot \rho v_2 \cdot \rho + 6(v_2 \cdot \rho)^2) - 4v_1 \cdot \rho v_1 \cdot \epsilon v_2 \cdot \epsilon(5\gamma v_1 \cdot \rho \\
& + 3v_2 \cdot \rho)]) - 12(5\gamma^2 - 7)|b|^4[v_1 \cdot \rho v_2 \cdot \epsilon - v_1 \cdot \epsilon(v_2 \cdot \rho)]^2, \tag{4.29a}
\end{aligned}$$

$$\begin{aligned}
W_{1,B^2} = & 120(\gamma^2 - 1)(b \cdot \epsilon[v_2 \cdot \rho - \gamma v_1 \cdot \rho] \\
& + u_1 v_1 \cdot \rho[\gamma v_1 \cdot \epsilon - v_2 \cdot \epsilon] + u_2 v_2 \cdot \rho[v_2 \cdot \epsilon - \gamma v_1 \cdot \epsilon]) \\
& \times (|b|^2[\gamma b \cdot \epsilon v_1 \cdot \rho + 3u_1 v_1 \cdot \rho v_2 \cdot \epsilon \\
& - \gamma u_1 v_1 \cdot \rho v_1 \cdot \epsilon - 3u_1 v_1 \cdot \epsilon v_2 \cdot \rho + \gamma u_2 v_1 \cdot \epsilon v_2 \cdot \rho] \\
& + 2(\gamma^2 - 1)u_1^2[u_1(-2v_1 \cdot \rho v_2 \cdot \epsilon + 3\gamma v_1 \cdot \rho v_1 \cdot \epsilon + 2v_1 \cdot \epsilon v_2 \cdot \rho) \\
& - 3\gamma(b \cdot \epsilon v_1 \cdot \rho + u_2 v_1 \cdot \epsilon v_2 \cdot \rho)]). \tag{4.29b}
\end{aligned}$$

We have confirmed this result agrees with the recent ref. [43].

From the complete waveform  $f^{(2)} = f_{\text{pp}}^{(2)} + f_{\text{tidal}}^{(2)}$  we may deduce both the radiated linear and angular momentum [78, 116]:

$$P_{\text{rad}}^\mu = \frac{1}{32\pi G} \int dud\sigma [\dot{f}_{ij}]^2 \rho^\mu, \quad \text{where } f = f_{ij} \epsilon^{ij}, \tag{4.30}$$

$$J_{ij}^{\text{rad}} = \frac{1}{8\pi G} \int dud\sigma \left( f_{k[i} \dot{f}_{j]k} - \frac{1}{2} x_{[i} \partial_{j]} f_{kl} \dot{f}_{kl} \right), \tag{4.31}$$

with  $\dot{f}_{ij} := \partial_u f_{ij}$  and  $d\sigma = \sin\theta d\theta d\phi$  the unit sphere measure. These formulae are most naturally interpreted in the center-of-mass frame — see ref. [49] for details. From (4.30) we confirm our expression (4.16) for  $P_{\text{rad}}^\mu$ , working up to  $\mathcal{O}(v^5)$  in a PN expansion in order to handle the difficult multi-scale integrals. As for the radiated angular momentum, at leading order in  $G$  this involves an integral over the gravitational wave memory, which vanishes at the current  $\mathcal{O}(G^2)$ :

$$\Delta f_{\text{tidal}}(\hat{\mathbf{x}}) := f_{\text{tidal}}(+\infty, \hat{\mathbf{x}}) - f_{\text{tidal}}(-\infty, \hat{\mathbf{x}}) = \mathcal{O}(G^3). \tag{4.32}$$

As explained in ref. [48], only diagrams with a deflection mode  $z_i^\mu$  propagating on a worldline contribute to the memory: this is not the case for the two diagrams in



Fig. 9. Hence the correction to  $J_{\text{rad}}$  from tidal effects begins at  $\mathcal{O}(G^3)$ , and using the linear response relation (4.15) this accounts for the fact that the radiative part of the scattering angle  $\theta_{\text{rad}}$  is unmodified by tidal effects until  $\mathcal{O}(G^4)$ .

## 5 Conclusions

In this paper we have introduced the Schwinger-Keldysh in-in formalism to the WQFT, defining complete (including radiation-reaction) scattering observables. This involved doubling the degrees of freedom in our action, with two evolution operators evolving states forwards and backwards in time between the observation point and past infinity. Our main observation is that calculating complete observables using WQFT with the in-in formalism boils down to a simple prescription: draw the sum of tree-level Feynman diagrams, with exactly the same Feynman rules as in the in-out prescription, but with *retarded propagators* all pointing towards the outgoing line representing the operator being measured. This ensures a flow of causality, so that when performing calculations there is no practical need to double degrees of freedom in the action.

This simplification is in no way surprising — indeed, it has been taken somewhat implicitly in previous work on the WQFT [47–51, 58]. From a purely classical perspective, one may view the sum over tree-level WQFT diagrams as simply a mechanism for solving the classical equations of motion of the theory — the approach taken in ref. [32] for solving classical electromagnetism, but there working in configuration rather than momentum space. Fixing boundary conditions at past infinity then requires the use of retarded propagators. This illustrates a key advantage of the WQFT over PM EFT-style methods [35, 37, 39, 40]: in the latter, integrating out the gravitons to leave an effective worldline action — separating bulk from worldline degrees of freedom — obscures the causal nature of the observables. While the need to double degrees of freedom in the action can still be cleverly avoided by focusing on specific radiative observables, such as the radiated four-momentum  $P_{\text{rad}}^\mu$  [42–44], we prefer a more flexible approach that produces complete observables.

We are left though with a practical question, which is the feasibility of performing loop integrals with retarded propagators. At first glance this seems a difficult task, given the apparent need to track signs on  $i0$  for all of our graviton propagators. However, this prescription is only relevant for *active propagators*: ones that can go on-shell over the domain of integration, and so for which the integration contour plays a meaningful role. In fact, at 3PM order there is no more than one active graviton propagator in any given integral (and none at all at 2PM order, which explains these integrals being rational functions). This simplifying property is the result of energy conservation on the worldlines, which restricts most graviton momenta to the potential region where  $\ell_i^{\text{pot}} = (\ell_i^0, \boldsymbol{\ell}_i) \sim (v, 1)$ .

Here there is an advantage of starting from the worldline rather than calculating observables using scattering amplitudes in the KMOC formalism [83, 84]. While it is tempting to assume that — upon taking the classical  $\hbar \rightarrow 0$  limit in the KMOC approach — the loop integrands obtained match those in the WQFT, the requirement of energy conservation is obscured from the amplitudes perspective. Using KMOC it is therefore more natural to adopt a Feynman-type basis, in which case the formalism also produces cut integrals. These cuts are unnecessary when using the WQFT because, essentially, the retarded propagators already contain them:

$$\frac{1}{k^2 + \text{sgn}(k^0)i0} = \frac{1}{k^2 + i0} + 2i\pi\theta(-k^0)\delta(k^2). \quad (5.1)$$

Furthermore, integrals with retarded propagators are purely *real* in the physical domain  $1 < \gamma < \infty$ , as compared with Feynman integrals that are (pseudo-)real only in the unphysical domain  $-1 < \gamma < 1$  [68, 80]. This makes sense, given that we seek real physical observables as linear combinations of these integrals.

To illustrate the Schwinger-Keldysh WQFT formalism we calculated complete gravitational observables in a scattering event involving two massive bodies including tidal corrections, including the momentum impulse  $\Delta p_1^\mu$ , scattering angle  $\theta$ , and radiated four-momentum  $P_{\text{rad}}^\mu$ . The latter two were also obtained recently using the worldline EFT formalism [43]. We observed that the tidal correction to the scattering angle is unmodified by the inclusion of radiation-reaction effects, which follows via the Bini-Damour linear response relation [78, 114, 115] from the absence of radiated angular momentum  $J_{\text{rad,tid}}$  at 2PM order. As confirmation we calculated the complete time-domain gravitational waveform at 2PM order from this scattering event, again reproducing the results of ref. [43], and confirming both the radiated linear and angular momentum at 3PM and 2PM orders respectively.

Our use of the Schwinger-Keldysh in-in formalism, and in particular our understanding of how to handle loop integrals with retarded propagators, paves the way to more advanced calculations in the future. A first step will be upgrading 3PM scattering observables involving quadratic-in-spin (quadrupole) effects, produced earlier this year by two of the present authors [51], to include radiation-reaction effects. Here the radiated four-momentum has been produced [44], but the full set of observables remains unknown. In the longer term, we see the WQFT as a powerful tool for performing 4PM calculations. Our aim will be to produce complete observables, thus avoiding any ambiguity between conservative and radiative contributions in the future.

## Acknowledgments

We would like to thank Gregor Kälin, Chia-Hsien Shen and Jan Steinhoff for very insightful discussions and comments on the manuscript. We also thank the organizers of the “High-Precision Gravitational Waves” program at the Kavli Institute

for Theoretical Physics (KITP) for their hospitality. GUJ's and GM's research is funded by the Deutsche Forschungsgemeinschaft (DFG, German Research Foundation), Projektnummer 417533893/GRK2575 "Rethinking Quantum Field Theory". This research was also supported in part by the National Science Foundation under Grant No. NSF PHY-1748958.

## A In-in propagator matrix

In order to derive the in-in propagator matrix we begin with the definition of the generating functional using the time-evolution operators in the free theory (2.9):

$$e^{\frac{i}{\hbar}W[J_1, J_2]} = \langle 0 | \hat{U}_{J_2}^{(0)}(-\infty, \infty) \hat{U}_{J_1}^{(0)}(\infty, -\infty) | 0 \rangle, \quad (\text{A.1})$$

with

$$\hat{U}_J^{(0)}(T', T) = \mathcal{T} \exp \left[ \frac{i}{\hbar} \int_T^{T'} dt \int d^3x \left( J(x) \hat{\phi}_I(x) \right) \right]. \quad (\text{A.2})$$

Taking a variational derivative of  $\hat{U}_J^{(0)}(T', T)$  with respect to  $J(x)$  inserts the field operator  $\hat{\phi}_I(x)$  into the time-ordered expression:

$$\frac{\hbar}{i} \frac{\delta \hat{U}_J^{(0)}(T', T)}{\delta J(t, \mathbf{x})} = \mathcal{T} \left( \hat{\phi}_I(t, \mathbf{x}) \exp \left[ \frac{i}{\hbar} \int_T^{T'} dt \int d^3x \left( J(x) \hat{\phi}_I(x) \right) \right] \right), \quad (\text{A.3})$$

and similarly for the anti-time ordered case ( $T > T'$ ). Similar relations hold for two functional derivatives. It is then straightforward to compute the propagator matrix via functional derivatives of the generating functional (A.1):

$$\langle \phi_A(x) \phi_B(y) \rangle = \frac{\delta^2 W[J_1, J_2]}{\delta J_B(y) \delta J_A(x)} \Big|_{J_a=0} = \frac{\delta^2 \langle 0 | \hat{U}_{J_2}^{(0)}(-\infty, \infty) \hat{U}_{J_1}^{(0)}(\infty, -\infty) | 0 \rangle}{\delta J_B(y) \delta J_A(x)} \Big|_{J_a=0}, \quad (\text{A.4})$$

where  $A, B = 1, 2$ . Using  $\langle 0 | 0 \rangle = 1$  one finds that

$$\begin{aligned} \langle \phi_1(x) \phi_1(y) \rangle &= \langle 0 | \mathcal{T} \phi(x) \phi(y) | 0 \rangle, & \langle \phi_1(x) \phi_2(y) \rangle &= \langle 0 | \phi(y) \phi(x) | 0 \rangle, \\ \langle \phi_2(x) \phi_1(y) \rangle &= \langle 0 | \phi(x) \phi(y) | 0 \rangle, & \langle \phi_2(x) \phi_2(y) \rangle &= \langle 0 | \mathcal{T}^* \phi(x) \phi(y) | 0 \rangle, \end{aligned} \quad (\text{A.5})$$

as quoted in eq. (2.12). From here it is an easy exercise to transform this into the Keldysh basis using  $\phi_+ = \frac{1}{2}(\phi_1 + \phi_2)$  and  $\phi_- = \phi_1 - \phi_2$ . To do so, one uses

$$\begin{aligned} D_{\text{ret}}(x, y) &= \theta(x^0 - y^0) \langle 0 | [\phi(x), \phi(y)] | 0 \rangle \\ &= D_F(x, y) - D_-(x, y) = D_+(x, y) - D_D(x, y), \\ D_{\text{adv}}(x, y) &= \theta(y^0 - x^0) \langle 0 | [\phi(x), \phi(y)] | 0 \rangle \\ &= D_F(x, y) - D_+(x, y) = D_-(x, y) - D_D(x, y), \end{aligned} \quad (\text{A.6})$$

and  $D_H(x, y) = \langle 0 | \{ \phi(x), \phi(y) \} | 0 \rangle$  to find that

$$\begin{aligned} \langle \phi_+(x) \phi_-(y) \rangle &= D_{\text{ret}}(x, y), & \langle \phi_-(x) \phi_+(y) \rangle &= -D_{\text{adv}}(x, y), \\ \langle \phi_+(x) \phi_+(y) \rangle &= \frac{1}{2} D_H(x, y), & \langle \phi_-(x) \phi_-(y) \rangle &= 0. \end{aligned} \quad (\text{A.7})$$

This precisely reproduces eq. (2.14).

## References

- [1] I. Newton, *Philosophiæ Naturalis Principia Mathematica*. England, 1687.
- [2] LIGO SCIENTIFIC, VIRGO, KAGRA collaboration, R. Abbott et al., *GWTC-3: Compact Binary Coalescences Observed by LIGO and Virgo During the Second Part of the Third Observing Run*, [2111.03606](#).
- [3] L. Blanchet, *Gravitational Radiation from Post-Newtonian Sources and Inspiralling Compact Binaries*, *Living Rev. Rel.* **17** (2014) 2 [[1310.1528](#)].
- [4] Schäfer, Gerhard and Jaranowski, Piotr, *Hamiltonian formulation of general relativity and post-Newtonian dynamics of compact binaries*, *Living Rev. Rel.* **21** (2018) 7 [[1805.07240](#)].
- [5] T. Futamase and Y. Itoh, *The post-Newtonian approximation for relativistic compact binaries*, *Living Rev. Rel.* **10** (2007) 2.
- [6] M. E. Pati and C. M. Will, *PostNewtonian gravitational radiation and equations of motion via direct integration of the relaxed Einstein equations. 1. Foundations*, *Phys. Rev. D* **62** (2000) 124015 [[gr-qc/0007087](#)].
- [7] L. Bel, T. Damour, N. Deruelle, J. Ibanez and J. Martin, *Poincaré-invariant gravitational field and equations of motion of two pointlike objects: The postlinear approximation of general relativity*, *Gen. Rel. Grav.* **13** (1981) 963.
- [8] T. Ledvinka, G. Schaefer and J. Bicak, *Relativistic Closed-Form Hamiltonian for Many-Body Gravitating Systems in the Post-Minkowskian Approximation*, *Phys. Rev. Lett.* **100** (2008) 251101 [[0807.0214](#)].
- [9] W. D. Goldberger and I. Z. Rothstein, *An Effective field theory of gravity for extended objects*, *Phys. Rev. D* **73** (2006) 104029 [[hep-th/0409156](#)].
- [10] W. D. Goldberger and I. Z. Rothstein, *Towers of Gravitational Theories*, *Gen. Rel. Grav.* **38** (2006) 1537 [[hep-th/0605238](#)].
- [11] W. D. Goldberger and A. Ross, *Gravitational radiative corrections from effective field theory*, *Phys. Rev. D* **81** (2010) 124015 [[0912.4254](#)].
- [12] B. Kol and M. Smolkin, *Non-Relativistic Gravitation: From Newton to Einstein and Back*, *Class. Quant. Grav.* **25** (2008) 145011 [[0712.4116](#)].
- [13] C. R. Galley and M. Tiglio, *Radiation reaction and gravitational waves in the effective field theory approach*, *Phys. Rev. D* **79** (2009) 124027 [[0903.1122](#)].
- [14] S. Foffa, P. Mastrolia, R. Sturani, C. Sturm and W. J. Torres Bobadilla, *Static two-body potential at fifth post-Newtonian order*, *Phys. Rev. Lett.* **122** (2019) 241605 [[1902.10571](#)].
- [15] J. Blümlein, A. Maier, P. Marquard and G. Schäfer, *The fifth-order post-Newtonian Hamiltonian dynamics of two-body systems from an effective field theory approach: potential contributions*, *Nucl. Phys. B* **965** (2021) 115352 [[2010.13672](#)].

- [16] D. Bini, T. Damour and A. Geralico, *Binary dynamics at the fifth and fifth-and-a-half post-Newtonian orders*, *Phys. Rev.* **D102** (2020) 024062 [[2003.11891](#)].
- [17] D. Bini, T. Damour and A. Geralico, *Sixth post-Newtonian nonlocal-in-time dynamics of binary systems*, *Phys. Rev.* **D102** (2020) 084047 [[2007.11239](#)].
- [18] B. Kocsis, M. E. Gaspar and S. Marka, *Detection rate estimates of gravity-waves emitted during parabolic encounters of stellar black holes in globular clusters*, *Astrophys. J.* **648** (2006) 411 [[astro-ph/0603441](#)].
- [19] S. Mukherjee, S. Mitra and S. Chatterjee, *Gravitational wave observatories may be able to detect hyperbolic encounters of black holes*, *Mon. Not. Roy. Astron. Soc.* **508** (2021) 5064 [[2010.00916](#)].
- [20] M. Zevin, J. Samsing, C. Rodriguez, C.-J. Haster and E. Ramirez-Ruiz, *Eccentric Black Hole Mergers in Dense Star Clusters: The Role of Binary–Binary Encounters*, *Astrophys. J.* **871** (2019) 91 [[1810.00901](#)].
- [21] R. Gamba, M. Breschi, G. Carullo, P. Rettengo, S. Albanesi, S. Bernuzzi et al., *GW190521: A dynamical capture of two black holes*, [2106.05575](#).
- [22] M. Khalil, A. Buonanno, J. Steinhoff and J. Vines, *Energetics and scattering of gravitational two-body systems at fourth post-Minkowskian order*, [2204.05047](#).
- [23] Kälin, Gregor and Porto, Rafael A., *From Boundary Data to Bound States*, *JHEP* **01** (2020) 072 [[1910.03008](#)].
- [24] Kälin, Gregor and Porto, Rafael A., *From boundary data to bound states. Part II. Scattering angle to dynamical invariants (with twist)*, *JHEP* **02** (2020) 120 [[1911.09130](#)].
- [25] G. Cho, G. Kälin and R. A. Porto, *From boundary data to bound states. Part III. Radiative effects*, *JHEP* **04** (2022) 154 [[2112.03976](#)].
- [26] K. S. Thorne and S. J. Kovacs, *The generation of gravitational waves. I. Weak-field sources.*, *Astrophys. J.* **200** (1975) 245.
- [27] R. J. Crowley and K. S. Thorne, *The generation of gravitational waves. II. The postlinear formation revisited.*, *Astrophys. J.* **215** (1977) 624.
- [28] S. Kovacs and K. Thorne, *The Generation of Gravitational Waves. 3. Derivation of Bremsstrahlung Formulas*, *Astrophys. J.* **217** (1977) 252.
- [29] S. Kovacs and K. Thorne, *The Generation of Gravitational Waves. 4. Bremsstrahlung*, *Astrophys. J.* **224** (1978) 62.
- [30] K. Westpfahl, *High-Speed Scattering of Charged and Uncharged Particles in General Relativity*, *Fortsch. Phys.* **33** (1985) 417.
- [31] S. E. Gralla and K. Lobo, *Self-force effects in post-Minkowskian scattering*, *Class. Quant. Grav.* **39** (2022) 095001 [[2110.08681](#)].

- [32] M. V. S. Saketh, J. Vines, J. Steinhoff and A. Buonanno, *Conservative and radiative dynamics in classical relativistic scattering and bound systems*, *Phys. Rev. Res.* **4** (2022) 013127 [[2109.05994](#)].
- [33] R. A. Porto, *The effective field theorist's approach to gravitational dynamics*, *Phys. Rept.* **633** (2016) 1 [[1601.04914](#)].
- [34] M. Levi, *Effective Field Theories of Post-Newtonian Gravity: A comprehensive review*, *Rept. Prog. Phys.* **83** (2020) 075901 [[1807.01699](#)].
- [35] Kälin, Gregor and Porto, Rafael A., *Post-Minkowskian Effective Field Theory for Conservative Binary Dynamics*, *JHEP* **11** (2020) 106 [[2006.01184](#)].
- [36] G. Cho, B. Pardo and R. A. Porto, *Gravitational radiation from inspiralling compact objects: Spin-spin effects completed at the next-to-leading post-Newtonian order*, *Phys. Rev. D* **104** (2021) 024037 [[2103.14612](#)].
- [37] Kälin, Gregor and Liu, Zhengwen and Porto, Rafael A., *Conservative Dynamics of Binary Systems to Third Post-Minkowskian Order from the Effective Field Theory Approach*, *Phys. Rev. Lett.* **125** (2020) 261103 [[2007.04977](#)].
- [38] Kälin, Gregor and Liu, Zhengwen and Porto, Rafael A., *Conservative Tidal Effects in Compact Binary Systems to Next-to-Leading Post-Minkowskian Order*, *Phys. Rev. D* **102** (2020) 124025 [[2008.06047](#)].
- [39] C. Dlapa, G. Kälin, Z. Liu and R. A. Porto, *Dynamics of binary systems to fourth Post-Minkowskian order from the effective field theory approach*, *Phys. Lett. B* **831** (2022) 137203 [[2106.08276](#)].
- [40] C. Dlapa, G. Kälin, Z. Liu and R. A. Porto, *Conservative Dynamics of Binary Systems at Fourth Post-Minkowskian Order in the Large-Eccentricity Expansion*, *Phys. Rev. Lett.* **128** (2022) 161104 [[2112.11296](#)].
- [41] S. Mougiakakos, M. M. Riva and F. Vernizzi, *Gravitational Bremsstrahlung in the post-Minkowskian effective field theory*, *Phys. Rev. D* **104** (2021) 024041 [[2102.08339](#)].
- [42] M. M. Riva and F. Vernizzi, *Radiated momentum in the post-Minkowskian worldline approach via reverse unitarity*, *JHEP* **11** (2021) 228 [[2110.10140](#)].
- [43] S. Mougiakakos, M. M. Riva and F. Vernizzi, *Gravitational Bremsstrahlung with tidal effects in the post-Minkowskian expansion*, [2204.06556](#).
- [44] M. M. Riva, F. Vernizzi and L. K. Wong, *Gravitational Bremsstrahlung from Spinning Binaries in the Post-Minkowskian Expansion*, [2205.15295](#).
- [45] J. S. Schwinger, *Brownian motion of a quantum oscillator*, *J. Math. Phys.* **2** (1961) 407.
- [46] L. V. Keldysh, *Diagram technique for nonequilibrium processes*, *Zh. Eksp. Teor. Fiz.* **47** (1964) 1515.

- [47] G. Mogull, J. Plefka and J. Steinhoff, *Classical black hole scattering from a worldline quantum field theory*, *JHEP* **02** (2021) 048 [[2010.02865](#)].
- [48] G. U. Jakobsen, G. Mogull, J. Plefka and J. Steinhoff, *Classical Gravitational Bremsstrahlung from a Worldline Quantum Field Theory*, *Phys. Rev. Lett.* **126** (2021) 201103 [[2101.12688](#)].
- [49] G. U. Jakobsen, G. Mogull, J. Plefka and J. Steinhoff, *Gravitational Bremsstrahlung and Hidden Supersymmetry of Spinning Bodies*, *Phys. Rev. Lett.* **128** (2022) 011101 [[2106.10256](#)].
- [50] G. U. Jakobsen, G. Mogull, J. Plefka and J. Steinhoff, *SUSY in the sky with gravitons*, *JHEP* **01** (2022) 027 [[2109.04465](#)].
- [51] G. U. Jakobsen and G. Mogull, *Conservative and Radiative Dynamics of Spinning Bodies at Third Post-Minkowskian Order Using Worldline Quantum Field Theory*, *Phys. Rev. Lett.* **128** (2022) 141102 [[2201.07778](#)].
- [52] L. J. Dixon, *Calculating scattering amplitudes efficiently*, in *Theoretical Advanced Study Institute in Elementary Particle Physics (TASI 95): QCD and Beyond*, 1, 1996, [hep-ph/9601359](#).
- [53] H. Elvang and Y.-t. Huang, *Scattering Amplitudes*, [1308.1697](#).
- [54] J. M. Henn and J. C. Plefka, *Scattering Amplitudes in Gauge Theories*, vol. 883. Springer, Berlin, 2014, [10.1007/978-3-642-54022-6](#).
- [55] Z. Bern, J. J. Carrasco, M. Chiodaroli, H. Johansson and R. Roiban, *The Duality Between Color and Kinematics and its Applications*, [1909.01358](#).
- [56] G. Travaglini et al., *The SAGEX Review on Scattering Amplitudes*, [2203.13011](#).
- [57] F. Bastianelli, F. Comberiati and L. de la Cruz, *Light bending from eikonal in worldline quantum field theory*, *JHEP* **02** (2022) 209 [[2112.05013](#)].
- [58] C. Shi and J. Plefka, *Classical double copy of worldline quantum field theory*, *Phys. Rev. D* **105** (2022) 026007 [[2109.10345](#)].
- [59] T. Wang, *Binary Dynamics from Worldline QFT for Scalar-QED*, [2205.15753](#).
- [60] D. Neill and I. Z. Rothstein, *Classical Space-Times from the S Matrix*, *Nucl. Phys. B* **877** (2013) 177 [[1304.7263](#)].
- [61] A. Luna, I. Nicholson, D. O’Connell and C. D. White, *Inelastic Black Hole Scattering from Charged Scalar Amplitudes*, *JHEP* **03** (2018) 044 [[1711.03901](#)].
- [62] N. Bjerrum-Bohr, J. F. Donoghue and P. Vanhove, *On-shell Techniques and Universal Results in Quantum Gravity*, *JHEP* **02** (2014) 111 [[1309.0804](#)].
- [63] N. J. Bjerrum-Bohr, P. H. Damgaard, G. Festuccia, L. Planté and P. Vanhove, *General Relativity from Scattering Amplitudes*, *Phys. Rev. Lett.* **121** (2018) 171601 [[1806.04920](#)].
- [64] Z. Bern, C. Cheung, R. Roiban, C.-H. Shen, M. P. Solon and M. Zeng, *Scattering*

- Amplitudes and the Conservative Hamiltonian for Binary Systems at Third Post-Minkowskian Order*, *Phys. Rev. Lett.* **122** (2019) 201603 [[1901.04424](#)].
- [65] Z. Bern, C. Cheung, R. Roiban, C.-H. Shen, M. P. Solon and M. Zeng, *Black Hole Binary Dynamics from the Double Copy and Effective Theory*, *JHEP* **10** (2019) 206 [[1908.01493](#)].
- [66] C. Cheung and M. P. Solon, *Classical gravitational scattering at  $\mathcal{O}(G^3)$  from Feynman diagrams*, *JHEP* **06** (2020) 144 [[2003.08351](#)].
- [67] N. E. J. Bjerrum-Bohr, P. H. Damgaard, L. Planté and P. Vanhove, *The amplitude for classical gravitational scattering at third Post-Minkowskian order*, *JHEP* **08** (2021) 172 [[2105.05218](#)].
- [68] P. Di Vecchia, C. Heissenberg, R. Russo and G. Veneziano, *The eikonal approach to gravitational scattering and radiation at  $\mathcal{O}(G^3)$* , *JHEP* **07** (2021) 169 [[2104.03256](#)].
- [69] Z. Bern, J. Parra-Martinez, R. Roiban, M. S. Ruf, C.-H. Shen, M. P. Solon et al., *Scattering Amplitudes and Conservative Binary Dynamics at  $\mathcal{O}(G^4)$* , *Phys. Rev. Lett.* **126** (2021) 171601 [[2101.07254](#)].
- [70] Z. Bern, J. Parra-Martinez, R. Roiban, M. S. Ruf, C.-H. Shen, M. P. Solon et al., *Scattering Amplitudes, the Tail Effect, and Conservative Binary Dynamics at  $\mathcal{O}(G^4)$* , *Phys. Rev. Lett.* **128** (2022) 161103 [[2112.10750](#)].
- [71] A. Guevara, A. Ochirov and J. Vines, *Scattering of Spinning Black Holes from Exponentiated Soft Factors*, *JHEP* **09** (2019) 056 [[1812.06895](#)].
- [72] A. Guevara, A. Ochirov and J. Vines, *Black-hole scattering with general spin directions from minimal-coupling amplitudes*, *Phys. Rev.* **D100** (2019) 104024 [[1906.10071](#)].
- [73] R. Aoude and A. Ochirov, *Classical observables from coherent-spin amplitudes*, *JHEP* **10** (2021) 008 [[2108.01649](#)].
- [74] W.-M. Chen, M.-Z. Chung, Y.-t. Huang and J.-W. Kim, *The 2PM Hamiltonian for binary Kerr to quartic in spin*, [2111.13639](#).
- [75] Z. Bern, D. Kosmopoulos, A. Luna, R. Roiban and F. Teng, *Binary Dynamics Through the Fifth Power of Spin at  $\mathcal{O}(G^2)$* , [2203.06202](#).
- [76] R. Aoude, K. Haddaxfd and A. Helset, *Searching for Kerr in the 2PM amplitude*, *JHEP* **07** (2022) 072 [[2203.06197](#)].
- [77] F. Febres Cordero, M. Kraus, G. Lin, M. S. Ruf and M. Zeng, *Conservative Binary Dynamics with a Spinning Black Hole at  $\mathcal{O}(G^3)$  from Scattering Amplitudes*, [2205.07357](#).
- [78] T. Damour, *Radiative contribution to classical gravitational scattering at the third order in  $G$* , *Phys. Rev. D* **102** (2020) 124008 [[2010.01641](#)].
- [79] P. Di Vecchia, C. Heissenberg, R. Russo and G. Veneziano, *Universality of*



- ultra-relativistic gravitational scattering*, *Phys. Lett. B* **811** (2020) 135924 [[2008.12743](#)].
- [80] E. Herrmann, J. Parra-Martinez, M. S. Ruf and M. Zeng, *Radiative classical gravitational observables at  $\mathcal{O}(G^3)$  from scattering amplitudes*, *JHEP* **10** (2021) 148 [[2104.03957](#)].
- [81] P. Di Vecchia, C. Heissenberg, R. Russo and G. Veneziano, *Radiation Reaction from Soft Theorems*, *Phys. Lett. B* **818** (2021) 136379 [[2101.05772](#)].
- [82] F. Alessio and P. Di Vecchia, *Radiation reaction for spinning black-hole scattering*, [2203.13272](#).
- [83] D. A. Kosower, B. Maybee and D. O’Connell, *Amplitudes, Observables, and Classical Scattering*, *JHEP* **02** (2019) 137 [[1811.10950](#)].
- [84] B. Maybee, D. O’Connell and J. Vines, *Observables and amplitudes for spinning particles and black holes*, *JHEP* **12** (2019) 156 [[1906.09260](#)].
- [85] A. Cristofoli, R. Gonzo, D. A. Kosower and D. O’Connell, *Waveforms from Amplitudes*, [2107.10193](#).
- [86] A. Cristofoli, R. Gonzo, N. Moynihan, D. O’Connell, A. Ross, M. Sergola et al., *The Uncertainty Principle and Classical Amplitudes*, [2112.07556](#).
- [87] A. Edison and M. Levi, *A tale of tails through generalized unitarity*, [2202.04674](#).
- [88] P. H. Damgaard, K. Haddad and A. Helset, *Heavy Black Hole Effective Theory*, *JHEP* **11** (2019) 070 [[1908.10308](#)].
- [89] A. Brandhuber, G. Chen, G. Travaglini and C. Wen, *Classical gravitational scattering from a gauge-invariant double copy*, *JHEP* **10** (2021) 118 [[2108.04216](#)].
- [90] R. Aoude, K. Haddad and A. Helset, *Tidal effects for spinning particles*, *JHEP* **03** (2021) 097 [[2012.05256](#)].
- [91] R. Aoude, K. Haddad and A. Helset, *Classical gravitational spinning-spinless scattering at  $\mathcal{O}(G^2S^\infty)$* , [2205.02809](#).
- [92] G. Kälin, J. Neef and R. A. Porto, *Radiation-Reaction in the Effective Field Theory Approach to Post-Minkowskian Dynamics*, [2207.00580](#).
- [93] R. D. Jordan, *Effective Field Equations for Expectation Values*, *Phys. Rev. D* **33** (1986) 444.
- [94] M. D. Schwartz, *Quantum Field Theory and the Standard Model*. Cambridge University Press, 3, 2014.
- [95] C. Heissenberg, *Infrared divergences and the eikonal exponentiation*, *Phys. Rev. D* **104** (2021) 046016 [[2105.04594](#)].
- [96] E. Herrmann, J. Parra-Martinez, M. S. Ruf and M. Zeng, *Gravitational Bremsstrahlung from Reverse Unitarity*, *Phys. Rev. Lett.* **126** (2021) 201602 [[2101.07255](#)].

- [97] N. E. J. Bjerrum-Bohr, P. H. Damgaard, L. Planté and P. Vanhove, *Classical gravity from loop amplitudes*, *Phys. Rev. D* **104** (2021) 026009 [[2104.04510](#)].
- [98] A. V. Smirnov, *Algorithm FIRE – Feynman Integral REduction*, *JHEP* **10** (2008) 107 [[0807.3243](#)].
- [99] T. Gehrmann and E. Remiddi, *Differential equations for two loop four point functions*, *Nucl. Phys. B* **580** (2000) 485 [[hep-ph/9912329](#)].
- [100] J. M. Henn, *Multiloop integrals in dimensional regularization made simple*, *Phys. Rev. Lett.* **110** (2013) 251601 [[1304.1806](#)].
- [101] M. Beneke and V. A. Smirnov, *Asymptotic expansion of Feynman integrals near threshold*, *Nucl. Phys. B* **522** (1998) 321 [[hep-ph/9711391](#)].
- [102] A. V. Smirnov and F. S. Chuharev, *FIRE6: Feynman Integral REduction with Modular Arithmetic*, *Comput. Phys. Commun.* **247** (2020) 106877 [[1901.07808](#)].
- [103] R. N. Lee, *Presenting LiteRed: a tool for the Loop InTEgrals REDuction*, [1212.2685](#).
- [104] R. N. Lee, *LiteRed 1.4: a powerful tool for reduction of multiloop integrals*, *J. Phys. Conf. Ser.* **523** (2014) 012059 [[1310.1145](#)].
- [105] P. Maierhöfer, J. Usovitsch and P. Uwer, *Kira—A Feynman integral reduction program*, *Comput. Phys. Commun.* **230** (2018) 99 [[1705.05610](#)].
- [106] J. Klappert, F. Lange, P. Maierhöfer and J. Usovitsch, *Integral reduction with Kira 2.0 and finite field methods*, *Comput. Phys. Commun.* **266** (2021) 108024 [[2008.06494](#)].
- [107] J. M. Henn, *Lectures on differential equations for Feynman integrals*, *J. Phys. A* **48** (2015) 153001 [[1412.2296](#)].
- [108] V. A. Smirnov, *Analytic tools for Feynman integrals*, vol. 250. 2012, [10.1007/978-3-642-34886-0](#).
- [109] T. Becher, A. Broggio and A. Ferroglia, *Introduction to Soft-Collinear Effective Theory*, vol. 896. Springer, 2015, [10.1007/978-3-319-14848-9](#), [[1410.1892](#)].
- [110] D. Bini, T. Damour and A. Geralico, *Scattering of tidally interacting bodies in post-Minkowskian gravity*, *Phys. Rev.* **D101** (2020) 044039 [[2001.00352](#)].
- [111] K. Haddad and A. Helset, *Tidal effects in quantum field theory*, *JHEP* **12** (2020) 024 [[2008.04920](#)].
- [112] C. Cheung and M. P. Solon, *Tidal Effects in the Post-Minkowskian Expansion*, *Phys. Rev. Lett.* **125** (2020) 191601 [[2006.06665](#)].
- [113] D. Amati, M. Ciafaloni and G. Veneziano, *Higher Order Gravitational Deflection and Soft Bremsstrahlung in Planckian Energy Superstring Collisions*, *Nucl. Phys.* **B347** (1990) 550.
- [114] D. Bini and T. Damour, *Gravitational radiation reaction along general orbits in the effective one-body formalism*, *Phys. Rev.* **D86** (2012) 124012 [[1210.2834](#)].

- [115] D. Bini, T. Damour and A. Gericco, *Radiative contributions to gravitational scattering*, *Phys. Rev. D* **104** (2021) 084031 [[2107.08896](#)].
- [116] B. Bonga and E. Poisson, *Coulombic contribution to angular momentum flux in general relativity*, *Phys. Rev. D* **99** (2019) 064024 [[1808.01288](#)].